

**GEOTECHNICAL ENGINEERING**

**RESEARCH ON STRENGTH-DEFORMABILITY-WATER PRESSURE  
RELATIONSHIPS FOR FAULTS IN DIRECT SHEAR**

**AD 747673**

by

R. E. Goodman

F. E. Heuzé

Y. Ohnishi

D D C  
RECEIVED  
SEP 5 1972  
REGULATIVE  
D.

Final Report on ARPA Contract H0210020 - Amount \$ 44,701

Effective Date : February 5, 1972

Termination Date : March 5, 1972

Principal Investigator : Prof. R.E. Goodman (415) 642-5525

Faculty Investigator : Dr. F.E. Heuzé (415) 642-4217

Sponsored by Advanced Research Projects Agency

ARPA Order No. 1579-Amend.2-Program Code No.1F10

APRIL 1972

DISTRIBUTION STATEMENT J

Approved for public release;  
Distribution Unlimited

**UNIVERSITY OF CALIFORNIA • BERKELEY**

Reproduced by  
**NATIONAL TECHNICAL  
INFORMATION SERVICE**  
U S Department of Commerce  
Springfield VA 22151

RESEARCH ON STRENGTH-DEFORMABILITY-WATER PRESSURE  
RELATIONSHIPS FOR FAULTS IN DIRECT SHEAR

Final Report on ARPA Contract H0210020

ERRATA SHEET

<u>Page</u>	<u>Line</u>	
i & 52	20	After rock types insert, <u>except for granite at high roughnesses</u>
i & 52	26	Change <u>an increase</u> to <u>a decrease</u>
3	19	Change <u>532</u> to <u>360</u>
13	6	Change <u>4, 5, and 6</u> to <u>7, 8, and 9</u>
41	16	Change <u>except at high values (say &gt;10)</u> to <u>at low normal stress values</u>
42	9 & 10	Change <u>3</u> to <u>2</u>
	12	Change <u>4</u> to <u>3</u>
	15	Insert <u>normal</u> before pressure
	15	The portion after the semicolon should read <u>the primary factor influencing <math>\delta</math> is R</u>
43	10	Delete <u>and</u>
	12	Should read <u>the no-dilation normal pressure is in excess of 1,500 psi</u>
45	21	Change <u>consistently</u> to <u>usually</u>

Unclassified

3200.8 (Att 1 to Encl 1)

Mar 7, 66

Security Classification

DOCUMENT CONTROL DATA - R & D		
<i>(Security classification of title, body of abstract and indexing annotation must be entered when the overall report is classified)</i>		
1. ORIGINATING ACTIVITY (Corporate author)		2a. REPORT SECURITY CLASSIFICATION
Geological Engineering		Unclassified
University of California, Berkeley		7b. GROUP
3. REPORT TITLE		
Research on Strength-Deformability-Water pressure Relationships for Faults in Direct Shear.		
4. DESCRIPTIVE NOTES (Type of report and inclusive dates)		
Final Report February 5, 1971 - March 5, 1972		
5. AUTHOR(S) (First name, middle initial, last name)		
R.E. Goodman, F.E. Heuzé, Y. Ohnishi		
6. REPORT DATE	7a. TOTAL NO. OF PAGES	7b. NO. OF REFS
April 1972	81	5
8a. CONTRACT OR GRANT NO.	9a. ORIGINATOR'S REPORT NUMBER(S)	
ARPA H0210020		
b. PROJECT NO.		
c.	9b. OTHER REPORT NO.'S (Any other numbers that may be assigned this report)	
d.		
10. DISTRIBUTION STATEMENT		
Distribution of this report is unlimited		
11. SUPPLEMENTARY NOTES		12. SPONSORING MILITARY ACTIVITY
		Military Geophysics Program. Advanced Research Projects Agency
13. ABSTRACT		
<p>A program of direct shear tests on samples of rock joints was initiated to gain an improved picture of the deformation and strength of jointed rock masses under load. The shear testing machine, developed under an NSF grant, and improved during this project, allows water pressure to be monitored in the joint plane during shearing. Seventy-two tests were conducted in this first year of an intended 3 year's program; artificial joints were created in two rock types--granite and sandstone-- with varying wall roughness, filling material thickness, and environmental conditions.</p> <p>Joints and faults exert controls on rock movement below ground and their weakness and deformability limit the "hardness" of underground sites. Furthermore, water pressure phenomena create difficulties for design and construction. This research has added to the technology basis to rational engineering with rock masses. In the work, basic phenomena of jointed rock are being examined experimentally for the first time permitting formulation of correct constitutive laws for joints that are vital to numerical and physical modelling. In continuation, tests with jacketed specimens having preconsolidated filler material are proposed. Experimental methods for these improvements in testing technique have now been developed.</p>		

DD FORM 1473  
NOV 65Unclassified  
Security Classification

A

Security Classification

14. KEY WORDS	LINK A		LINK B		LINK C	
	ROLL	WT	ROLL	WT	ROLL	WT
Direct Shear Tests						
Faults						
Granite						
Gouge Material						
Joint Dilatancy						
Joint Roughness						
Joint Stiffness						
Joint Strength						
Joint Waviness						
Kaolinite						
Sandstone						
Water Pressure						

Unclassified

Security Classification

B

Geotechnical Engineering

RESEARCH ON STRENGTH-DEFORMABILITY-WATER PRESSURE  
RELATIONSHIPS FOR FAULTS IN DIRECT SHEAR

by

R. E. Goodman  
F. E. Heuzé  
Y. Ohnishi

Final Report - Contract ARPA No. H0210020 - Amount \$44,701  
Effective Date: February 5, 1971 - Termination Date: March 5, 1972

Principal Investigator: Professor R. E. Goodman (415) 642-5525  
Co-Investigator: Dr. F. E. Heuzé (415) 642-5525

Sponsored by Advanced Research Projects Agency  
ARPA Order No. 1579 - Amend. 2 - Program Code 1F10

Monitored by U.S. Bureau of Mines; T. Bur Project Officer

The views and conclusions contained in this document are those of the authors and should not be interpreted as necessarily representing the official policies either expressed or implied of the Advanced Research Projects Agency or the U. S. Government.

April 1972

University of California, Berkeley

SUMMARY OF TECHNICAL REPORT

A program of direct shear tests on samples of rock joints was initiated to gain an improved picture of the deformation and strength of jointed rock masses under load. The shear testing machine, developed under an NSF grant, and improved during this project, allows water pressure to be monitored in the joint plane during shearing. Seventy-two tests were conducted in this first year of an intended 3 year's program; artificial joints were created in two rock types -- granite and sandstone -- with varying wall roughness, filling material thickness, and environmental conditions.

The methods of preparing joint specimens of varying roughness were developed in this project; rough artificial joints were manufactured by splitting the specimens and smooth joints by diamond sawing and lapping. It was difficult to fill the joints to a predetermined thickness with gouge preconsolidated to a desired high normal pressure; remoulded gouge was therefore introduced. Roughness measurements were made and statistical parameters of roughness and waviness were computed using two specially written programs to be found in Appendices B and C. Typical test records are also given in the Appendix.

Table 7 summarizes the sensitivity of deformability and strength parameters to the variables studied. For the sandstone and granite specimens, both peak displacement and joint stiffness varied with normal pressure. The dilation angle decreased rapidly with normal pressure for both rock types and became negative for the sandstone specimens at  $\sigma$  above 500 psi (i.e. the specimens contracted during shear). Induced water pressures measured were not large (<25 psi), possibly due to the problem of sampling water pressures in the joint plane, partly due to the remoulded nature of the filling, and partly because of decay of the water pressure transients in the unjacketed specimens. Dilatant joints generally suffered an increase in pressure while contractant joints underwent a pore pressure buildup. Complete saturation of the joints was obtained, as

evidenced by the insensitivity of the results to chamber back pressure. Filled joints approached the strength of the clay filling material when the thickness was greater than about 3 times the mean roughness amplitude.

Joints and faults exert controls on rock movement below ground and their weakness and deformability limit the "hardness" of underground sites. Furthermore, water pressure phenomena create difficulties for design and construction. This research has added to the technology basic to rational engineering with rock masses. In the work, basic phenomena of jointed rock are being examined experimentally for the first time permitting formulation of correct constitutive laws for joints that are vital to numerical and physical modelling. In continuation, tests with jacketed specimens having preconsolidated filler material are proposed. Experimental methods for these improvements in testing technique have now been developed.

## PREFACE

This research was conducted by the Geological Engineering Group of the University of California, Berkeley. The Principal Investigator was Dr. Richard E. Goodman, Associate Professor of Geological Engineering. Co-Investigator was Dr. Francois E. Heuzé, Lecturer and Assistant Research Engineer in Geological Engineering. They were assisted by Mr. Yuzo Ohnishi, Research Assistant, to plan, perform and analyze the test program.

Additional personnel who contributed to this research are Mr. Quentin Gorton who developed and modified testing equipment in the first part of the research, assisted by Mr. John Walsh, and Mr. Mariano de Angulo who conducted studies of filler material consolidation and pore pressure development in clay material.

Miss Wanda Brandon typed the manuscript.

INDEX

	<u>Page</u>
SUMMARY OF TECHNICAL REPORT	i
PREFACE	iii
LIST OF FIGURES	vi
LIST OF TABLES	vii
<u>PART I: INTRODUCTION - OBJECTIVES</u>	
1. NATURE OF THE PROGRAM	1
2. PRINCIPLES INVOLVED - JOINT MECHANICS	1
a. The Direct Shear Test for Rock Joints	
b. Parameters of Joint Behavior	
3. PROGRAM PLAN AND VARIABLES	3
<u>PART II: METHOD OF INVESTIGATION</u>	
1. EQUIPMENT	12
2. SPECIMEN PREPARATION	13
a. Cutting and Potting	
b. Roughness and Waviness Measurements	
c. Filling Material	
3. TESTING PROCEDURE	15
4. PRACTICAL DIFFICULTIES	16
a. Jacketing of Specimens	
b. Water Pressure Measurement	
c. Filler Material	
d. Normal Stiffness Measurements	
<u>PART III: RESULTS OF THE TEST PROGRAM</u>	
1. PROPERTIES OF THE "GRANITE" AND THE SANDSTONE	28
a. Petrographic Examination	
b. Strength-Deformability and Bulk Properties	
2. ROUGHNESS AND WAVINESS OF THE JOINT PLANES	28
a. Roughness	
b. Waviness	
3. THICKNESS OF JOINT FILLER	28
4. DEFORMABILITY AND STRENGTH DATA	29
5. WATER PRESSURE DATA	30

## Index (Continued)

PagePART IV: DISCUSSION OF THE TEST RESULTS

- |   |    |
|---|----|
| 1. DISCUSSION OF JOINT DEFORMABILITY    | 41 |
| a. Sandstone Joints                     |    |
| b. Granite Joints                       |    |
| 2. DISCUSSION OF JOINT STRENGTH         | 43 |
| 3. DISCUSSION OF WATER PRESSURE RESULTS | 45 |

PART V: SUMMARY-CONCLUSIONS

- |  |    |
|--|----|
| REFERENCES   | 54 |
| APPENDIX A - PETROGRAPHY AND MINERALOGY OF THE PROJECT'S<br>ROCK TYPES     | 55 |
| APPENDIX B - ROUGHNESS ANALYSIS PROGRAM, AND SAMPLE OUTPUT<br>FOR TEST #61 | 60 |
| APPENDIX C - WAVINESS ANALYSIS PROGRAM, AND SAMPLE OUTPUT<br>FOR TEST #61  | 68 |
| APPENDIX D - TYPICAL TEST RECORD (TEST #61)                                | 74 |
| APPENDIX E - DOD DOCUMENT CONTROL DATA - R & D                             | 79 |

LIST OF FIGURES

	<u>Page</u>	
FIG. 1	Normal displacement of discontinuity under changing normal stress with constant shear stress	9
FIG. 2	Shear displacement under changing shear stress with constant normal stress	10
FIG. 3b	Actual dilation rates at different normal stresses	11
FIG. 4	36-Inch saw assembly	19
FIG. 5	Drill and vise assembly	20
FIG. 6	Roughness measuring system on mill table	21
FIG. 7	Direct shear machine, top removed	22
FIG. 8	Shear testing assembly and controls	23
FIG. 9	Normal loading device and regulator system	24
FIG. 10	Electronic data recording system	25
FIG. 11	Outline of testing procedure for direct shear tests	26
FIG. 12	Shear specimen assembled for testing (legend in text)	27
FIG. 13	Half specimen lay-out for roughness measurement	27
FIG. 14	Roughness distribution of sandstone joints	38
FIG. 15	Roughness distribution of granite joints	38
FIG. 16	Average slope angle vs. length of observation on joint planes	39
FIG. 17	Maximum positive slope angle vs. roughness of joint planes	39
FIG. 18	Dimensionless filler thickness ( $T_f/R$ ) for sandstone joints	40
FIG. 19	Dimensionless filler thickness for granite joints	40
FIG. 20	Peak strength of sandstone specimens	47
FIG. 21	Residual strength of sandstone specimens	48
FIG. 22	Peak strength of wet granite specimens	49
FIG. 23	Residual strength of wet granite	50
FIG. 24	Strength data for clay filled joints	51
FIG. 25	Record of test #61	78

LIST OF TABLES

	<u>Page</u>
TABLE 1: The test program	4
TABLE 2: Number of tests on each rock type used to analyze the influence of the various parameters, on the strength and deformability of the joints	8
TABLE 3: Summary of index properties for the rock types of the shear program	31
TABLE 4: Strength and deformability data for tests of the shear program	32
TABLE 5: Normal stiffness values for selected tests on filled joints	30
TABLE 6: Water pressures observed for tests on sandstone and granite joints	35
TABLE 7: Influence of the test program variables on joint deformability parameters	37

PART I: INTRODUCTION - OBJECTIVES

1. NATURE OF THE PROGRAM

The manner and rate of rock movements virtually control the cost of excavation, support, and operation underground. Rock movements, in turn, are largely dictated by the behavior of seams, joints, and faults which tend to destroy continuity of the rock mass. Methods of physical model study and finite element analysis make it possible to simulate the behavior of discontinuities in an engineering study of a particular underground scheme. However, very little is known about the relevant properties of the seams and joints. Existing knowledge on the methods of sampling and testing discontinuities in the laboratory and in the field was recently summarized by Goodman, (1970). The state of knowledge is unsatisfactory in that almost no attention has been paid to the development of water pressures during the shearing process. It is apparent that water plays an important role underground. This research project explores the effect of system and environmental conditions on stiffness and strength properties for artificial discontinuities. Direct shear tests were made on prepared specimens containing a known clay, filling the space between two rock walls under conditions of restricted drainage. Stresses, deformations and water pressures were monitored during the tests.

2. PRINCIPLES INVOLVED - JOINT MECHANICS

a. The Direct Shear Test for Rock Joints

Mathematical modelling of jointed rock masses requires quantitative assessment of the constitutive law for joints. This entails finding every acceptable combination of terms for the vector  $\langle u, v, \tau, \sigma \rangle$  where:  $u$  and  $v$  are the relative shear and normal displacements across the joint; and  $\tau$  and  $\sigma$  are respectively the shear and normal stress across the joint. One can speak of a

joint constitutive law as  $f(u, v, \tau, \sigma) = 0$ .

The most direct method of defining the joint constitutive law is to test a specimen representative of the joint surface, and filling material. The sample is oriented in a machine under circumstances wherein the normal and shear stress and displacement, and the environmental conditions are directly controlled or monitored. The direct shear machine is the natural method of achieving this. Direct shear, in fact, is the classical test conducted by workers in friction. For shear through continuous materials such as soils, the triaxial test is considered to provide more uniform stress conditions on the eventual failure plane. However, for rock specimens containing joints oriented in the plane of direct shear, Kutter (1971) showed the direct shear test to be preferable.

#### b. Parameters of Joint Behavior

The deformability and strength relationships of seams and joints can be described by direct shear testing. The relationship between ( $\tau$ ) and resulting shear displacement ( $u$ ) developed in the test is expressed in a curve which can be modelled in a physical study or in a digital computer by reporting the changing slopes at different stress levels. The rate of change  $(\partial\tau/\partial u)_\sigma$  is called the shear stiffness of the joint. Similarly, the closure of the joint specimen upon application of normal load provides a curve of increasing slope relating normal stress ( $\sigma$ ) to normal displacement ( $v$ ). The rate of change  $(\partial\sigma/\partial v)_\tau$  at any point is the instantaneous normal stiffness. During shearing there is also a tendency for joint thickening (dilation) or closing (contraction), which can be expressed by the rate of change  $(\partial\tau/\partial v)_\sigma$ . As a result of dilation the volume of the filling material in the sheared zone would tend to change; under conditions of restricted drainage, this tendency would immediately be resisted by the inertia of the water in the sheared zone; the cleft water therefore may suffer an increase or decrease from its original pressure level.

Obviously such a pressure change can be significant in describing the response of the sample to further loading or to the maintenance of existing loads.

It is probable that pore pressure changes are at the core of some stability and support problems both underground and at the surface. Figures 1, 2, and 3, show the form of the constitutive relationship assumed by Goodman and Dubois (1972). The parameters to be evaluated by a test program in addition to the strength parameters and the stiffness terms defined above, are: The maximum closure; normal pressure ( $\sigma_T$ ) above which dilatancy cannot occur; and the ratio of residual and peak shear strengths. Of special interest here are the effects of water and water pressure on these joint parameters.

### 3. PROGRAM PLAN AND VARIABLES

The full range of testing parameters consisted of:

- 2 rock types: granite and sandstone
- 3 roughness ranges for the sandstone and 2 for the granite
- 3 thickness ranges for the filling of the joints
- 2 shear rates (0.1 and 0.28 in./min)
- 4 back pressures (0, 200, 400 and 600 psi)
- 3 normal loads (100, 500 and 1,500 psi)

All combinations of the above parameters represent 532 possibilities. Considering the limitations in time and expenditures of this project, a balanced program of 72 tests was finally selected. Test numbers and parameter values are presented in table 1. Table 2 indicates the total number of tests performed on each rock type and how many of these were used to analyze the influence of the various parameters on the strength and deformability of the joints. This question is taken up again in the discussion of Part IV.

TABLE 1: The Test Program

TEST NO.	ROCK TYPE	JOINT TYPE	ROUGH. (10 <sup>-3</sup> IN)	SHEAR RATE	$\sigma_N$ (psi)	$P_b$ (psi)	$T_i$ (10 <sup>-2</sup> IN)	$\frac{T_i}{\text{ROUGHN.}}$
1	SANDSTONE	DRY	4.9	$\frac{1}{=0.1}$ in/min	100	-	-	-
2	"	"	45.7	1	1,500	-	-	-
3	"	"	1.9	1	1,500	-	-	-
4	"	"	8.1	1	1,500	-	-	-
5	"	"	1.7	1	1,500	-	-	-
6	"	"	10.4	1	500	-	-	-
7	"	"	27.3	1	500	-	-	-
8	"	"	1.8	1	100	-	-	-
9	"	"	1.5	1	500	-	-	-
10	"	"	4.7	1	500	-	-	-
11	"	"	9.9	1	100	-	-	-
12	"	WET	35.9	1	100	600	-	-
13	"	"	27.5	1	500	600	-	-
14	"	"	12.7	1	100	600	-	-
15	"	"	12.4	1	500	600	-	-
16	"	"	1.1	1	100	600	-	-
17	"	"	2.8	1	500	600	-	-
18	"	"	7.3	1	1,500	600	-	-
19	"	"	6.5	$\frac{1}{2}$	500	200	-	-
20	"	"	7.9		500	200	-	-
21	"	"	35.6	1	1,500	600	-	-
22	"	"	1.8	1	1,500	600	-	-

TABLE 1: The Test Program

TEST NO.	ROCK TYPE	JOINT TYPE	ROUGH. (10 <sup>-3</sup> IN)	SHEAR RATE	$\sigma_N$ (psi)	$P_b$ (psi)	$T_1$ (10 <sup>-2</sup> IN)	$\frac{T_1}{\text{ROUGHN.}}$
23	SANDSTONE	WET	14.2	2	1,500	200	-	-
24	"	"	18.0	1	1,000	200	-	-
25	"	FILLED	75.2	1	100	0	8.9	1.18
26	"	"	56.0	1	100	400	7.4	1.32
27	"	"	10.2	1	500	200	1.7	1.66
28	"	"	7.9	1	100	400	1.0	1.26
29	"	"	8.4	2	500	200	0.8	0.10
30	"	"	7.3	2	500	400	0.4	0.055
31	"	"	7.2	1	1,500	200	18.2	25.3
32	"	"	8.0	1	1,500	400	4.5	5.6
33	"	"	17.4	2	1,500	200	3.1	1.78
34	"	"	41.8	1	1,500	400	1.3	0.31
35	"	"	32.1	1	500	0	6.8	2.12
36	"	"	41.1	1	500	400	7.8	1.90
37	"	"	50.7	1	1,500	0	3.7	0.73
38	"	"	9.9	2	1,500	400	0.4	0.40
39	"	"	8.1	1	500	0	2.1	2.52
40	"	"	8.1	1	1,000	0	3.8	4.69
41	"	"	12.6	1	500	200	3.0	2.38
42	"	"	8.9	2	500	200	2.6	2.92
43	"	"	9.8	2	500	400	2.6	2.65
44	"	"	6.6	1	1,500	200	5.2	7.80

TABLE 1: The Test Program

TEST NO.	ROCK TYPE	JOINT TYPE	ROUGH. (10 <sup>-3</sup> IN)	SHEAR RATE	$\sigma_N$ (psi)	$P_b$ (psi)	$T_i$ (10 <sup>-2</sup> IN)	$\frac{T_i}{\text{ROUGHN.}}$
45	SANDSTONE	FILLED	6.4	2	1,500	200	4.3	6.72
46	"	"	8.7	2	1,500	400	7.8	8.95
47	"	"	8.2	1	100	0	2.1	2.56
48	GRANITE	DRY	65.5	1	500	-	-	-
49	"	"		1	500	-	-	-
50	"	WET	0.9	1	500	200	-	-
51	"	"	1.9	1	500	600	-	-
52	"	"	67.2	1	500	200	-	-
53	"	"	99.4	1	500	600	-	-
54	"	"	0.9	1	1,500	200	-	-
55	"	"	1.7	1	1,500	500	-	-
56	"	"	76.5	2	500	600	-	-
57	"	"	60.3	1	1,500	600	-	-
58	"	"	56.3	1	1,500	200	-	-
59	"	FILLED	1.1	1	500	200	4.2	38.2
60	"	"	1.1	1	500	600	4.7	42.8
61	"	"	51.6	1	500	200	7.2	1.39
62	"	"	117.5	1	500	400	5.1	0.43
63	"	"	1.4	1	1,500	200	2.9	20.7
64	"	"	2.9	1	1,500	600	4.6	15.9
65	"	"	50.5	2	500	400	4.6	0.91

TABLE 1: The Test Program

TEST NO.	ROCK TYPE	JOINT TYPE	ROUGH. ( $10^{-3}$ IN)	SHEAR RATE	$\sigma_N$ (psi)	$P_b$ (psi)	$T_1$ ( $10^{-2}$ IN)	$\frac{T_1}{\text{ROUGHN.}}$
66	GRANITE	FILLED	66.4	1	500	400	7.3	1.10
67	"	"	66.2	1	1,500	200	2.0	0.31
68	"	"	63.5	1	1,500	400	1.0	0.16
69	"	"	52.5	1	100	400	5.8	1.10
70	"	"	59.4	2	500	400	5.4	0.91
71	"	"	89.4	1	500	0	4.8	0.54
72	"	"	2.3	1	100	400	4.2	18.2

Table 2  
 Number of Tests on Each Rock Type Used to Analyze  
 the Influence of the Various Parameters, on the Strength  
 and Deformability of the Joints

Sandstone: 47 Tests

Granite: 25 Tests

	Normal Load	Roughness	Thickness	Chamber Pressure	Shear Rate
<b>Sandstone</b>					
$K_{ss}$	47	21	18	29	27
$\tau_p/\tau_r$	44	22	22	33	27
$u_p$	47	23	18	18	18
$\delta$	47	25	22	-	-
<b>Granite</b>					
$K_{ss}$	20	8	12	16	5
$\tau_p/\tau_r$	19	9	10	21	9
$u_p$	20	8	12	13	8
$\delta$	22	7	15	-	-

$K_{ss}$ : shear stiffness

$\tau_p/\tau_r$ : ratio of peak shear stress to residual shear stress

$u_p$ : shear displacement at peak stress

$\delta$ : dilatation angle

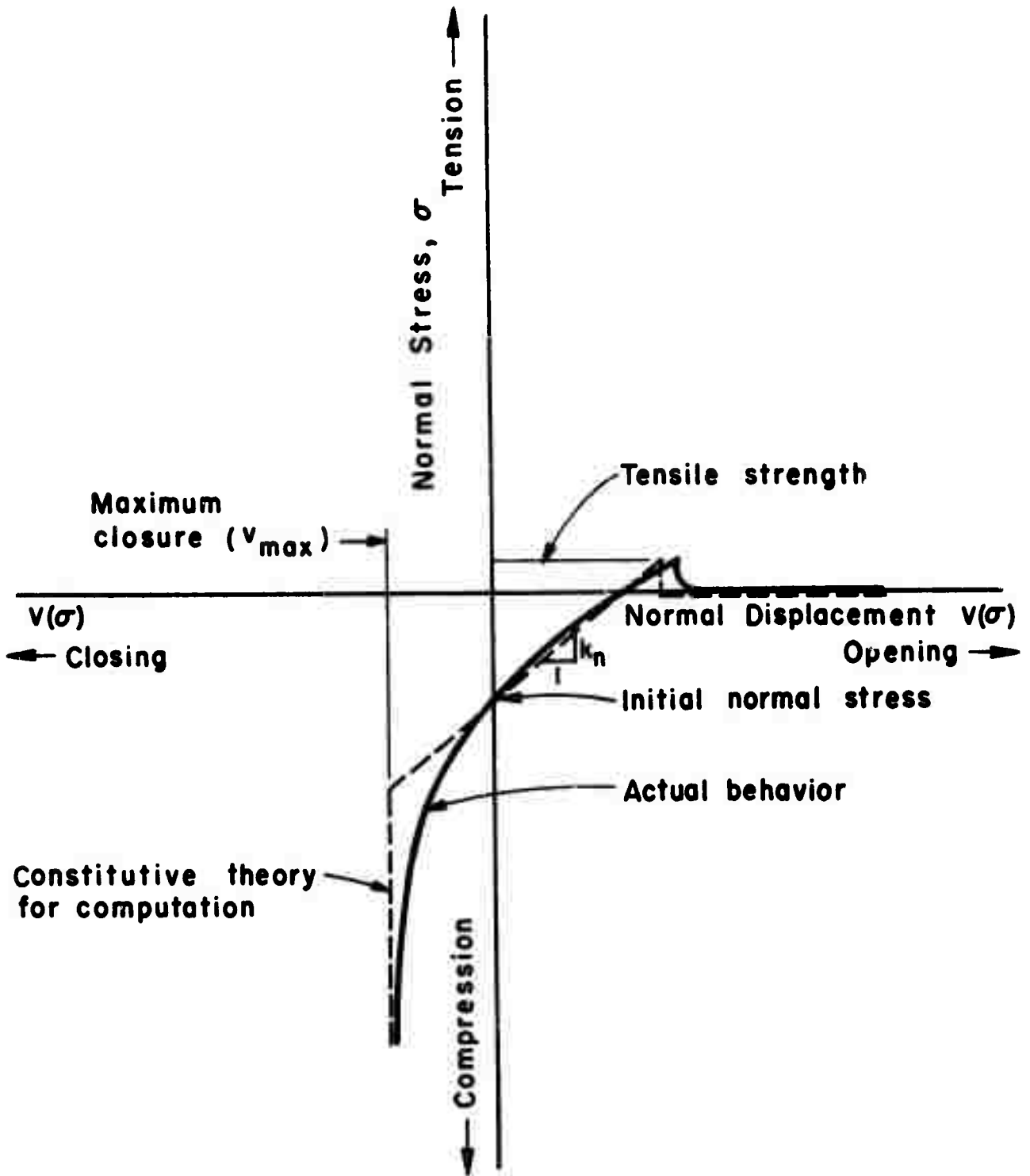


Figure 1. Normal displacement of discontinuity under changing normal stress with constant shear stress

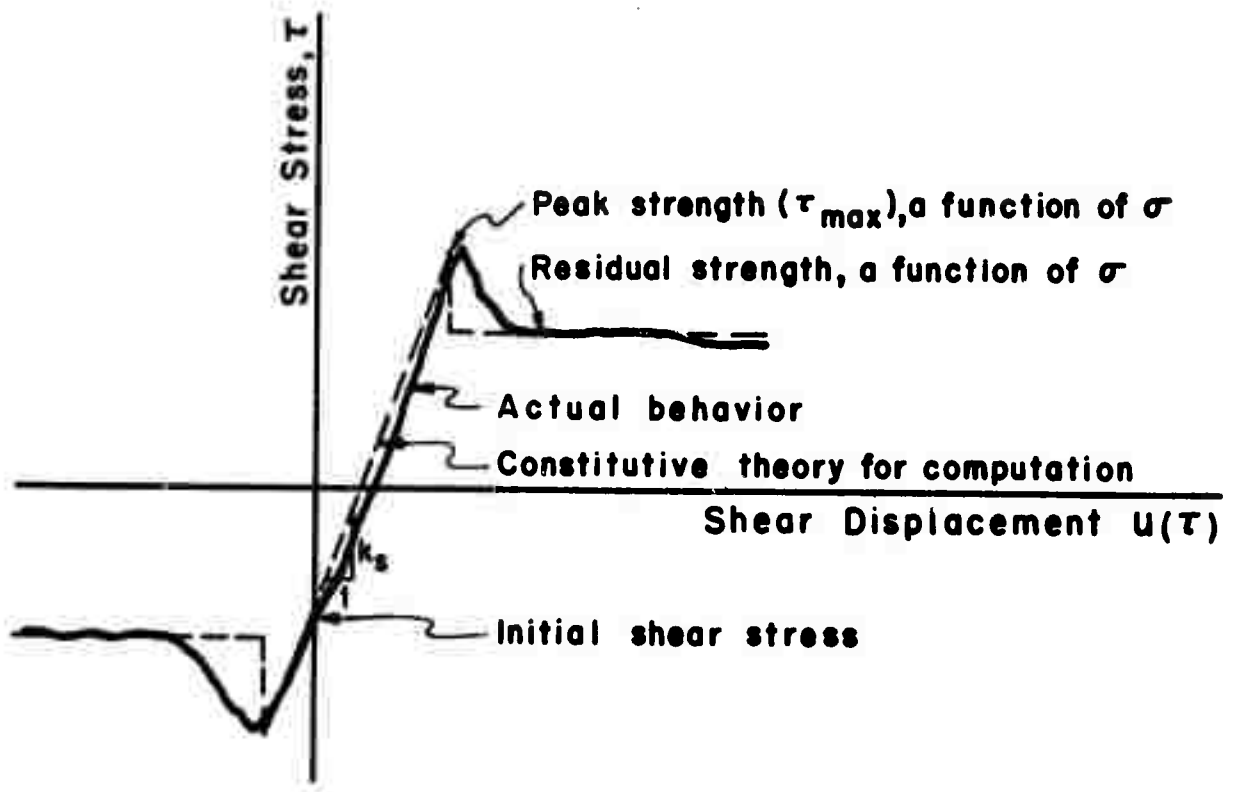


Figure 2. Shear displacement under changing shear stress with constant normal stress

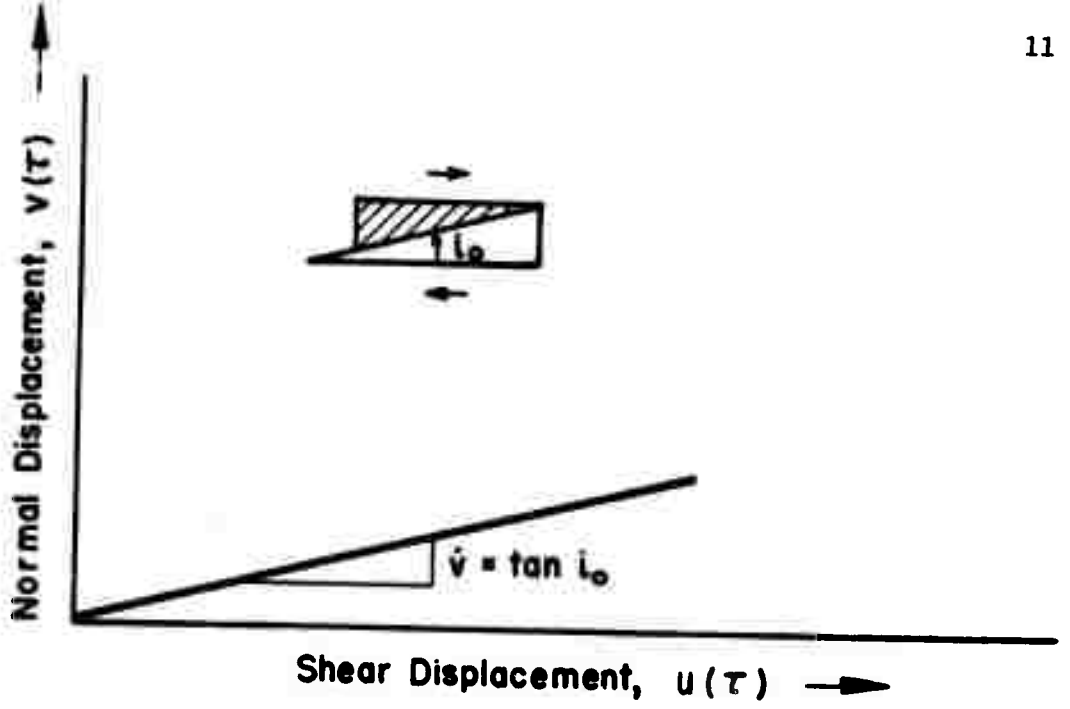


Figure 3a. Initial dilation rate at low normal stress

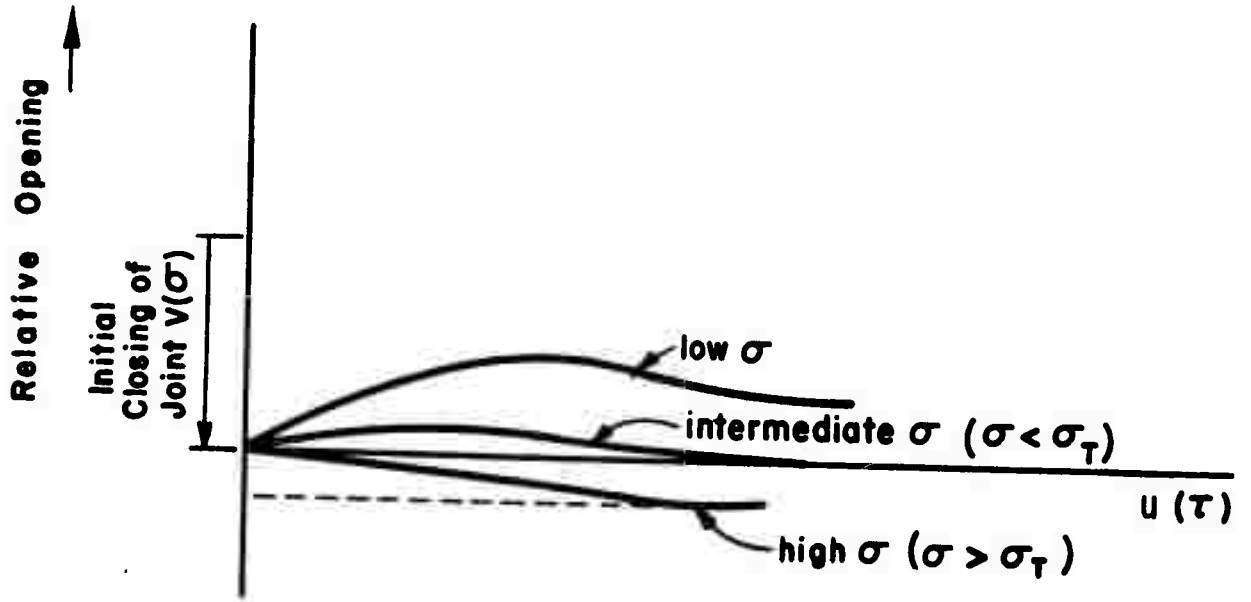


Figure 3b. Actual dilation rates at different normal stresses

12

## PART II: METHOD OF INVESTIGATION

### 1. EQUIPMENT

The equipment and supplies required for the performance of shear tests include: A large diamond saw for cutting of slabs or prisms (figure 4); a drill and vise assembly for drilling of cores to be tested for index properties (figure 5); a set of shear boxes with appropriate potting compound to set the specimens in their box; a roughness measuring device (figure 6); a direct shear assembly composed of shear machine (figures 7 and 8) and a normal load frame (figure 9); and a data acquisition system (figure 10).

The shear machine can provide shear loads of up to 40,000 lbs. The maximum shear displacement is 3 inches. The sample is contained within a sealed chamber that can sustain an internal water pressure of up to 700 psi; the shear box accommodates samples up to 5 x 5 in. in size. The normal load system is capable of sustaining a load of 40,000 lbs. It was redesigned so that a constant load level can be maintained within  $\pm 3/16$  in; this is the maximum normal displacement allowed with the shearing device. The load regulation is achieved by means of an oil/air accumulator of sufficiently large capacity. In practice, piston friction gives a finite stiffness to the normal load system.

Design of a direct shear machine is simple in concept. One provides known loads normal and parallel to the shear plane. Unfortunately rotational tendencies between members of the sample-shear box system cause non uniformities in the stress distribution. As the centroid of the joint contact area moves, the load center should follow it. This can be arranged easily, for example as in the Imperial College shear machine by applying normal loads through a hanging yoke; however, one would then complicate the problem of sealing a water chamber around the specimen. In fact each shear machine represents a compromise of specifications aimed at a particular region of excellence at

the expense of others; e.g. the University of Illinois machine can develop true residual friction values but cannot handle very large specimens and does not have water pressure control in the joint plane; the Berkeley machine was designed for water pressure control, but cannot accommodate large displacements to reach true residual strength for many joint types as the normal load is stationary. Figures 4, 5 and 6 show the shear machine, the controls and the normal loading system. The sample, up to 5-in square, is cemented in a steel box which is under-sheared by two screw driven pistons. The pistons crawl on a track on a rigid support as to prevent vertical movement. Therefore the lower half of the sample can move only horizontally. Vertical movement, but no horizontal movement, is allowed in the upper half of the sample, which carries the water chamber up and down as the joint dilates or contracts. The normal load is supplied by a hydraulic piston. The load is held constant, except for varying piston friction, using an accumulator precharged from a nitrogen bottle to the desired pressure.

The electronic bench is composed of: An amplifier/power supply module made by Kenney Engineering Co., (manufacturer of the direct shear machine); a digital voltmeter and relay matrix (NLS); a 7-channel printer (NLS); and an X-Y-Y' plotter.

The following test variables are monitored by transducers attached to the shear machine: Normal load ( $\sigma_n$ ); shear stress ( $\tau$ ); normal displacement ( $v$ ); shear displacement ( $u$ ); chamber water pressure ( $P$ ); and differential water pressures ( $p_1$  or  $p_2$ ) in the joint. Thus the printer enables recording of all variables simultaneously and the plotter enables monitoring of two variations at a time such as normal and shear stiffness, or pore pressure and dilatancy etc.

## 2. SPECIMEN PREPARATION

An outline of the testing procedure for direct shear tests is given in

figure 11. The upper half of the diagram represents the steps involved in preparing the specimen.

a. Cutting and Potting

One first cuts a prism of rock 4.75 x 4.75 x 2.75 in. in dimension. Then, depending upon the type of roughness desired for the joint plane the specimen is either

1. sawed in two: roughnesses 1 for granite and sandstone
2. sawed in two and sandblasted: roughness 2 for sandstone
3. split in two: roughness 2 for granite and 3 for sandstone.

It was found that polishing either granite or sandstone would not give a roughness much different from roughness 1. Values of roughness shown in table 1, indicate that this mode of preparation was successful in establishing definite classes of roughness values. The next step consists in potting the sample, as follows (figure 12): The bottom half of the specimen is put into the bottom half shear box and levelled by means of stiff levelling blocks (1). There may or may not be a filler material for the joint. The circumference of the joint surface (3) is protected by a bond breaker ( simple masking tape) and the two halves are potted separately by pouring the potting compound (cylcap, primarily sulphur) from holes in the bottom of the boxes, (2) and (4). The bond breaker insures that there will be no sulphur in the shearing plane. Two piezometric holes are then drilled up to the shear plane through guide holes in the bottom half box. These holes will connect, inside the shear chamber, with the water lines and pressure transducers.

b. Roughness and Waviness Measurements

After potting, samples are mounted on the table of the mill shown in figure 6. Micrometers enable precise location of the measuring points. Vertical elevations are obtained by means of a dial gage of sensitivity  $10^{-4}$  in. Eighty-one points are measured on the joint surface (figure 13). The data are

analyzed in terms of roughness and waviness of the surface. The two computer programs used for this analysis were prepared by Mr. Ohnishi and are presented in Appendices B and C with sample outputs. The following information is provided: The mean plane of the observations  $z = a_0 + a_1x + a_2y$ ; an estimate of the standard deviation from the mean plane  $\bar{\Delta z}$  -- this is called the roughness of the joint; the maximum positive and negative deviations from the mean plane (peaks and troughs); the average of positive slopes and of negative slopes between points at several distances -- 0.5, 1, 1.5, 2, 2.5, 3, 3.5 and 4 in; the maximum positive and negative slopes for these observations, on the above distances. All slopes are evaluated in the direction of shearing. Values are given in Part III for roughness and waviness.

### c. Filling Material

The choice of thickness for the filling material was guided by the roughness measured previously. Three ranges of dimensionless thickness values ( $T_1/R$  = initial thickness at beginning of shear/roughness) were obtained for the sandstone and two for the granite; values are presented in Part III.

The filling material first selected was the San Francisco Bay mud. However its composition is quite complex and grain size range is quite large. There was no certainty of obtaining a reproducible joint. Accordingly, a kaolinite clay with controlled properties was finally adopted. It is characterized by the following values (after Houston, 1967):

liquid limit 57%	plastic limit 30%
plasticity index 27%	percent $<2\mu = 100\%$
specific gravity 2.64	activity 0.30

Its expected strength envelope in C-U tests is shown on figure 24).

### 3. TESTING PROCEDURE

The various steps involved in the performance of a test are described in the lower portion of the diagram on figure 11. With wet tests unfilled or

or with filled joints, the specimens were first saturated, so that developing water pressures would not dissipate in the rock matrix during shear. Filled joints were coated with the kaolinite and their thickness at a normal load equal to that at the beginning of shear was measured in a separate hydraulic press, for maximum accuracy. Each test on filled joints was run in three subtests: 1) application of normal load, and determination of normal stiffness, with continuous plot of  $u$  and  $v$  vs.  $\sigma_n$ ; 2) application of the back pressure and saturation of the joint plane; 3) shearing -- in this subtest discrete readings were taken of all seven channels  $\sigma_n$ ,  $\tau$ ,  $P$ ,  $p_1$ ,  $p_2$ ,  $u$  and  $v$ . In addition continuous plots were obtained on the two x-y-y' plotters:  $u$  and  $v$  vs.  $\tau$  on the first one and  $p_1$  and  $p$  vs.  $\tau$  on the second one.

#### 4. PRACTICAL DIFFICULTIES

##### a. Jacketing of Specimens

Water pressures that would tend to build up during shearing would dissipate by flow away from the joint plane 1) through the wall rock and 2) into the chamber along the edges of the joint. The former can be prevented by using impervious wall rock for the test program; the latter can be prevented by jacketing the specimen. As originally proposed, jacketing would not be incorporated in the test program unless proved necessary as it introduces complexities in specimen preparation, sealing, saturation, and instrumentation. Jacketing is now being done in a continuation of the work, but all tests in the program described here were with unjacketed specimens.

##### b. Water Pressure Measurement

Since the volume of water in the joint space is small, the stiffness of the water pressure measuring system has an effect on the measurements. Initially, there was too much compressibility in long lines and Bourdon gages. These deficiencies were corrected by moving a differential transducer closer to the specimen. The transducer responds to pressure sources where the

measuring hole intersects the joint plane. This point was not always situated optimally within the joint; in continuation work underway, a distribution network to conduct pressure to the piezometer holes is being evaluated.

### c. Filler Material

Ideally, filler material in joints should be natural clay gouge or mylonite of the required thickness preconsolidated to the proper preconsolidation pressure. We do not know what to take as a reasonable value of preconsolidation pressure for a filled shear zone. This is an important parameter. Normally loaded clays can develop induced pore water pressures at peak shear displacement of the order of 40% of the preconsolidation pressure whereas remoulded clays may develop no induced pore pressure at all. Mylonites may be more like remoulded clays than normally consolidated clays.

Attempts to produce shear specimens with normally preconsolidated filling material of predetermined thickness were unsuccessful. Under conditions of only lateral drainage, the required load increment time for consolidation proved large; without multiple consolidometer arrangements the required number of samples therefore could be produced only by accepting considerable delay in the program. Attempts to speed up the consolidation process were frustrated by extrusion of clay from the joint. Instead of preconsolidated filling, therefore, remoulded clay was used. Also, as a substitute for natural gouge, an artificial kaolinite was selected for filling so that uniformity and homogeneity could be insured. However as kaolinite is representative of some faults and seams and no single clay gouge material can be representative of all faults and seams, the use of kaolinite for filler is appropriate.

### d. Normal Stiffness Measurements

To measure the normal stiffness of the joint, one must subtract the

shortening of the sample without a joint from that of the sample with a joint. Since the measurement utilizes the difference of large numbers, errors can be large unless care is taken to insure that the samples and procedures are in all respects the same except for the existence of the joint. Because of the many faceted nature of the experimental program, it was not convenient to meet this restraint in all tests, and therefore the program did not generally yield good results for normal stiffness values.

Reproduced from  
best available copy.

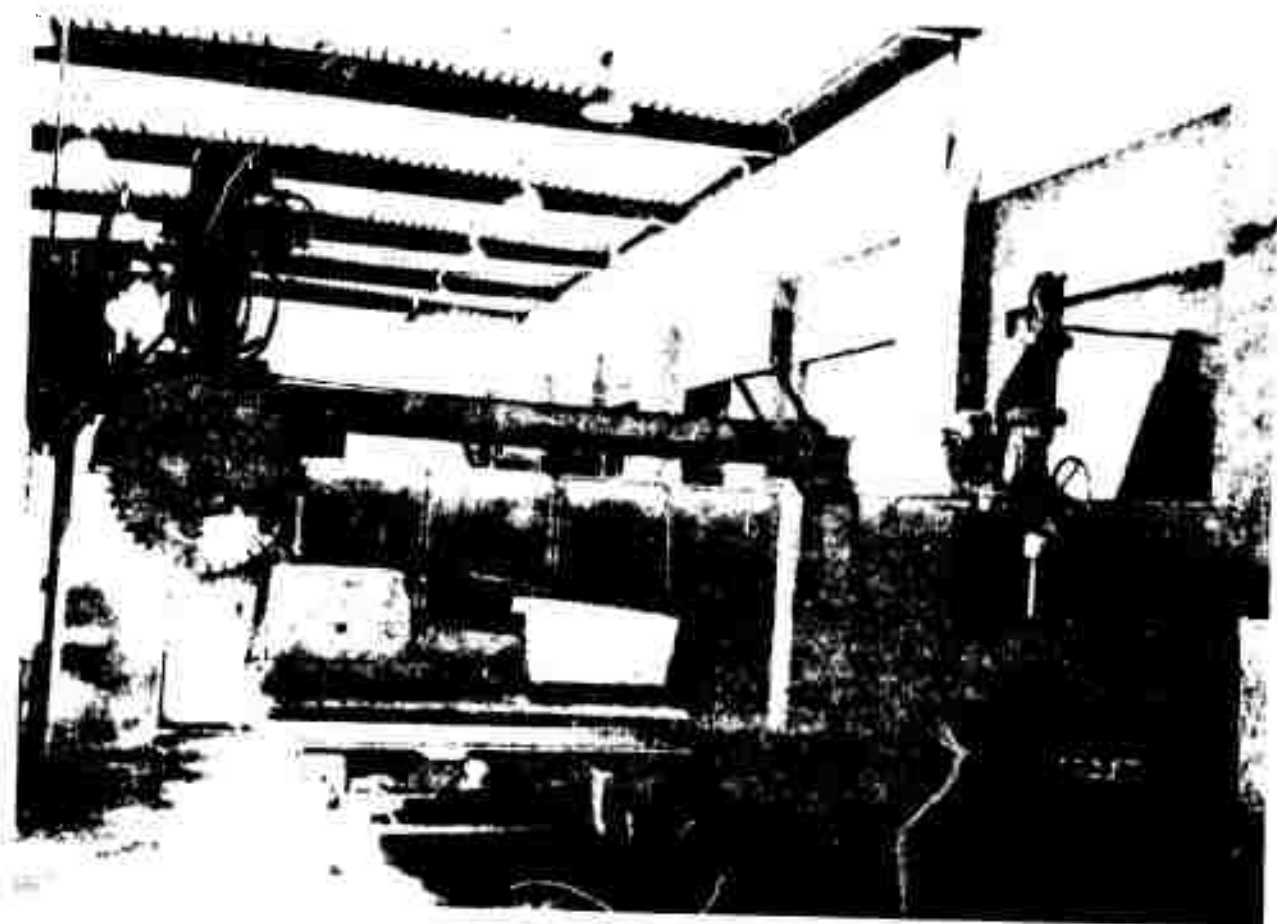


FIGURE 4 : 36-INCH SAW ASSEMBLY

Reproduced from  
best available copy.

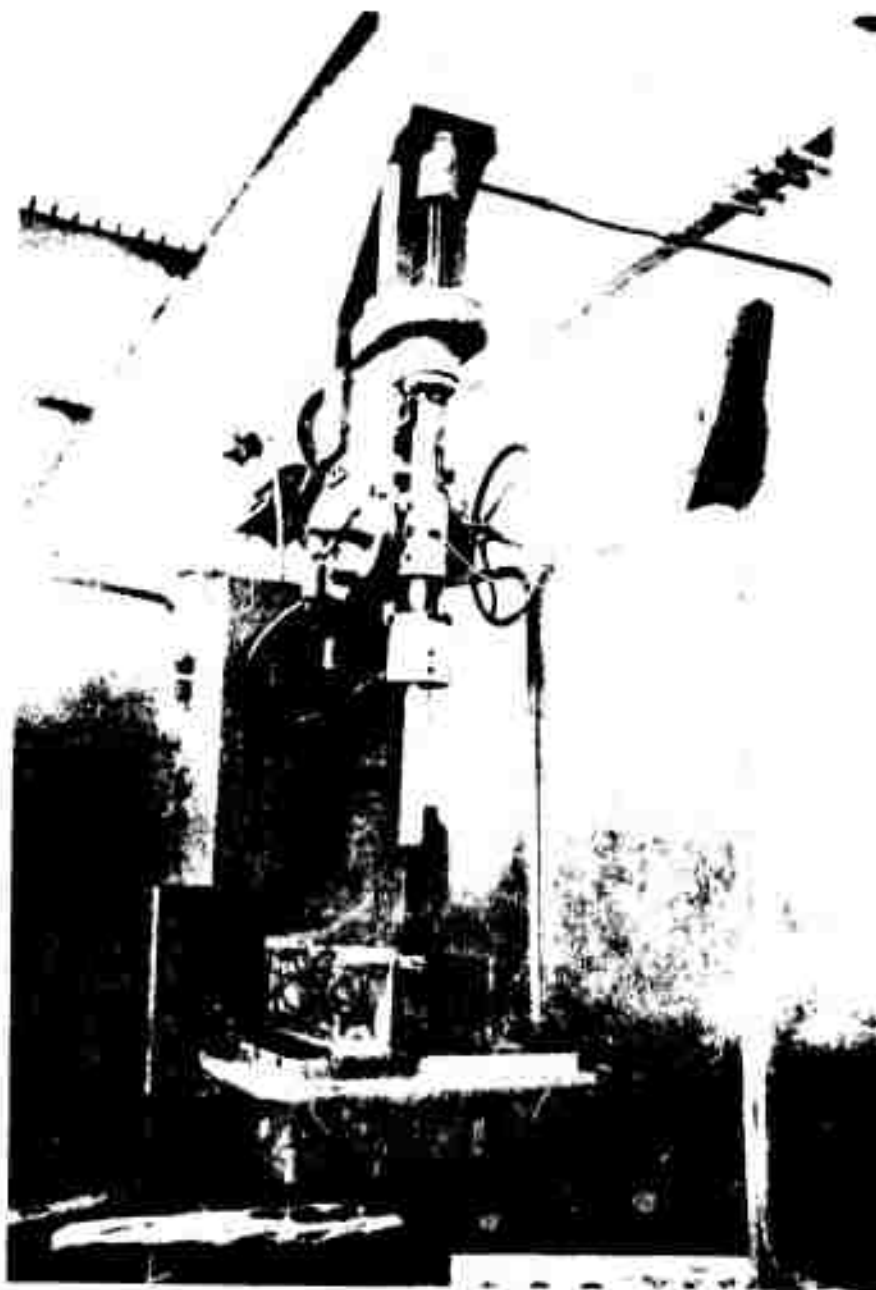


FIGURE 5 : DRILL AND VISE ASSEMBLY

Reproduced from  
best available copy.

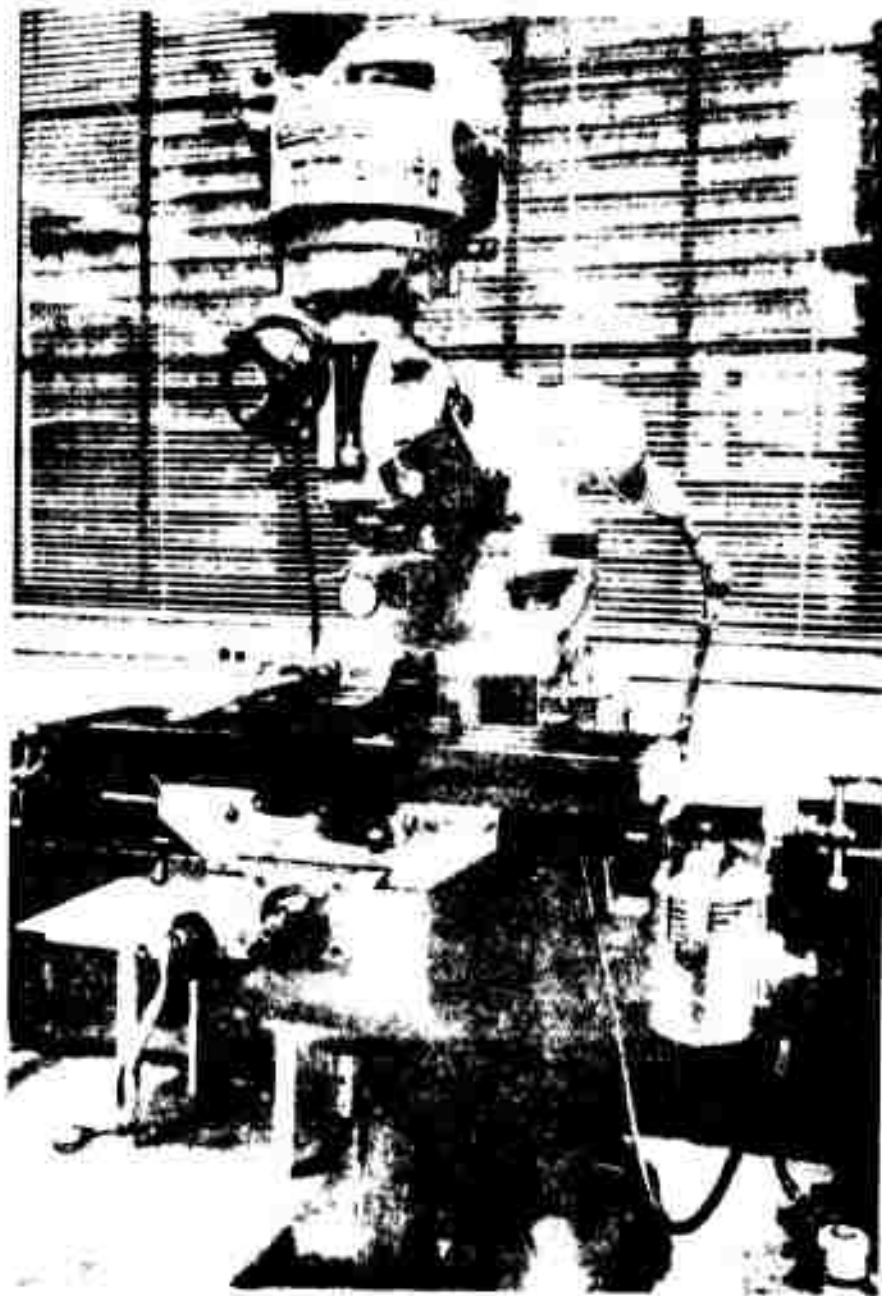


FIGURE 6: ROUGHNESS MEASURING SYSTEM ON MILL TABLE

Reproduced from  
best available copy.

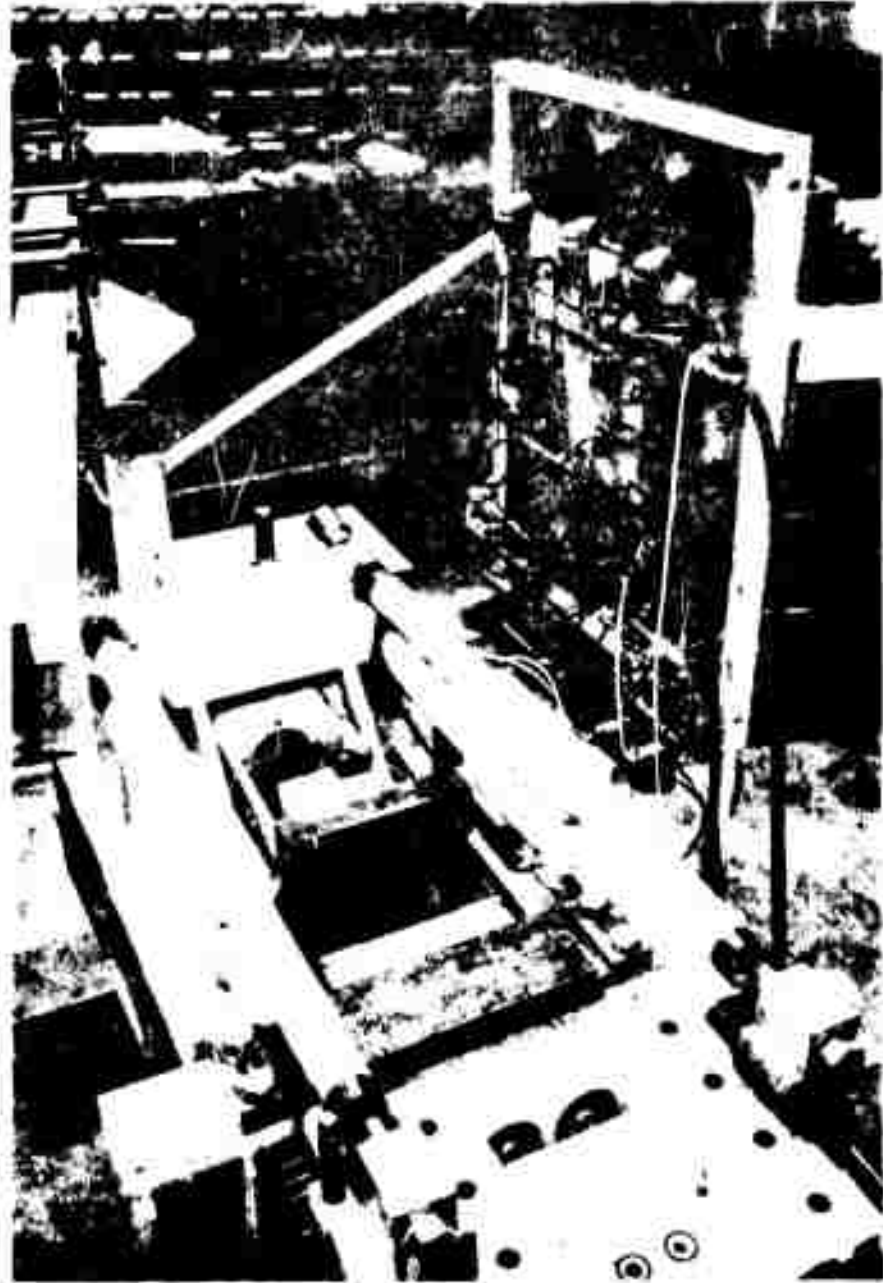


FIGURE 7 : DIRECT SHEAR MACHINE , TOP REMOVED

Reproduced from  
best available copy.

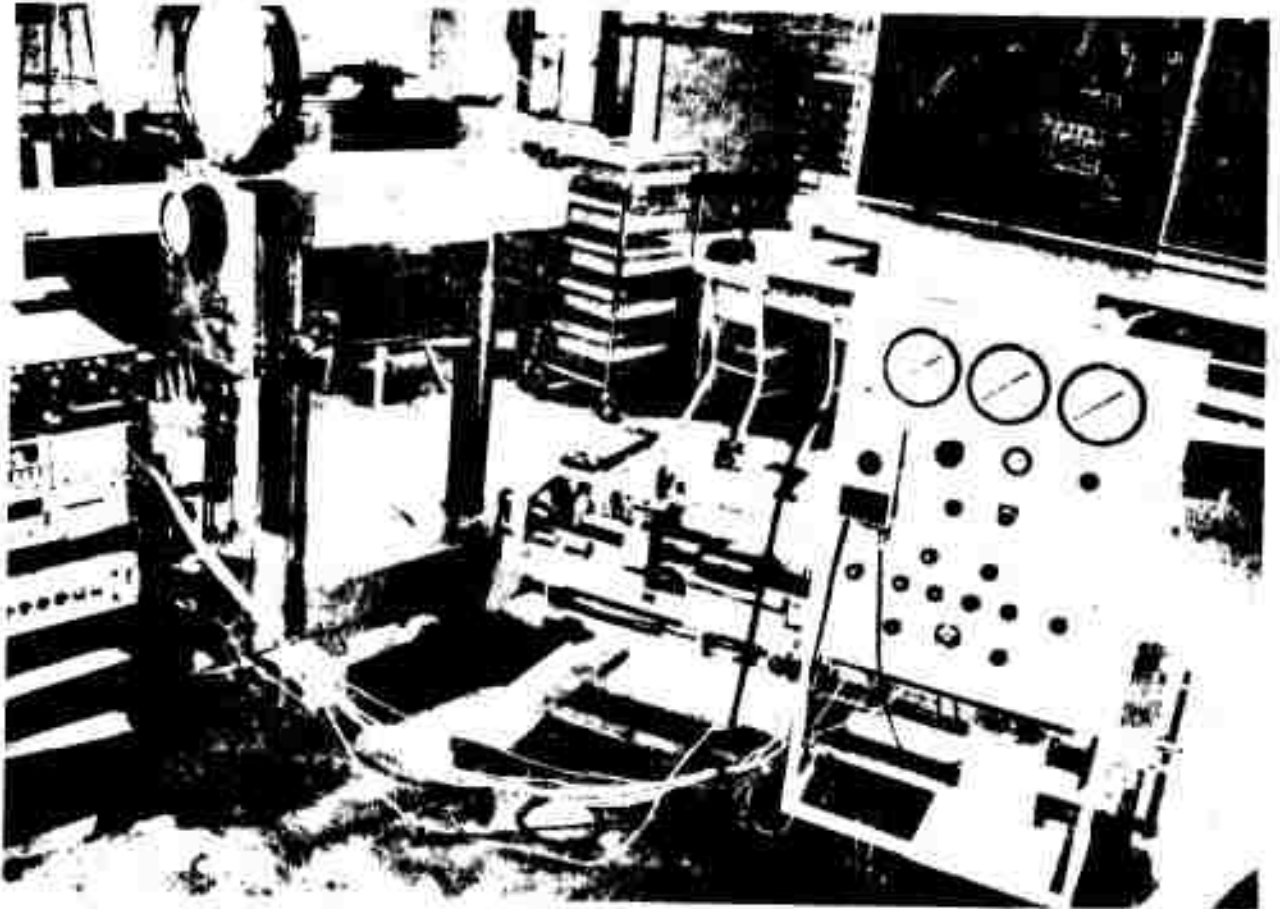


FIGURE 8 : SHEAR TESTING ASSEMBLY AND CONTROLS

Reproduced from  
best available copy.

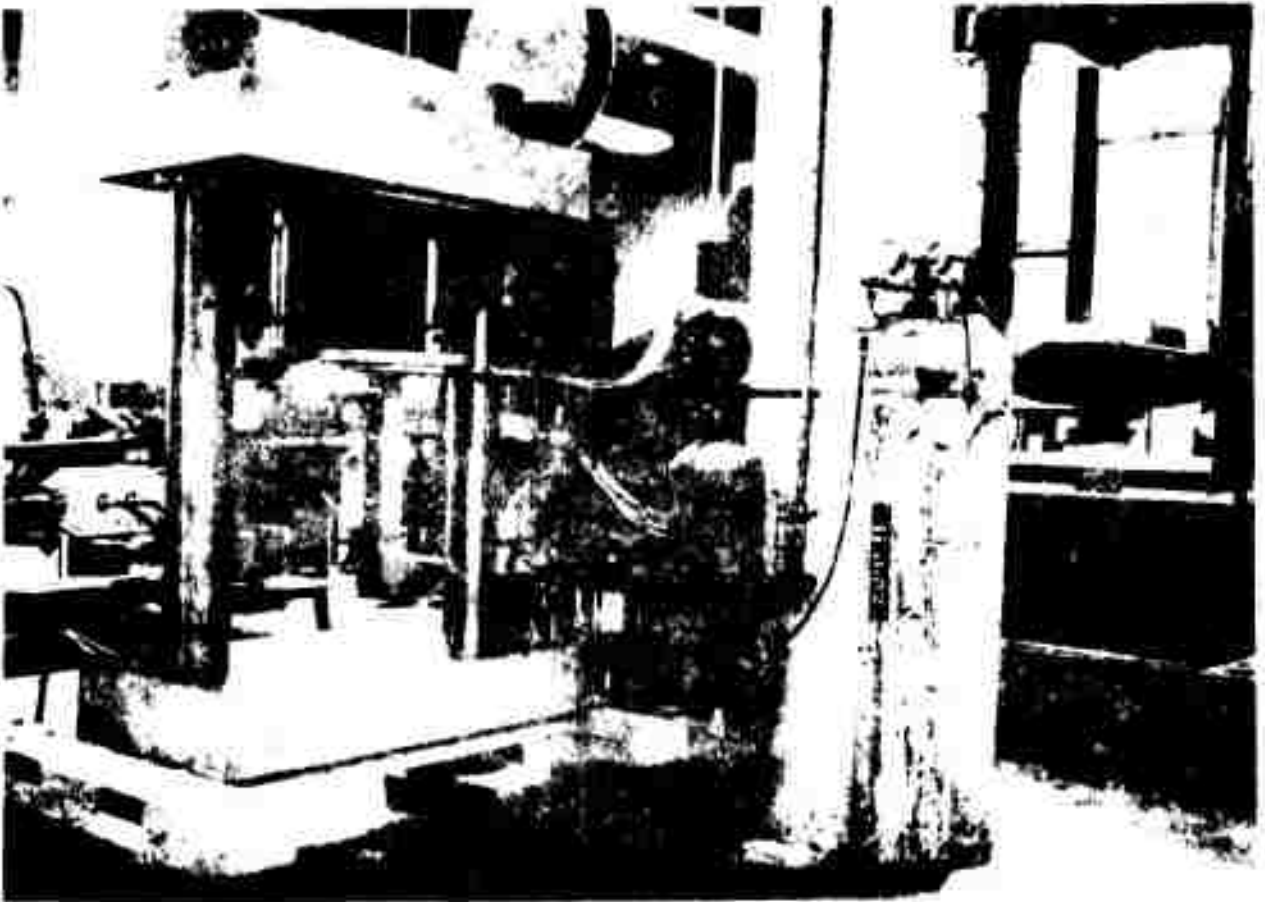


FIGURE 9 : NORMAL LOADING DEVICE AND REGULATOR SYSTEM

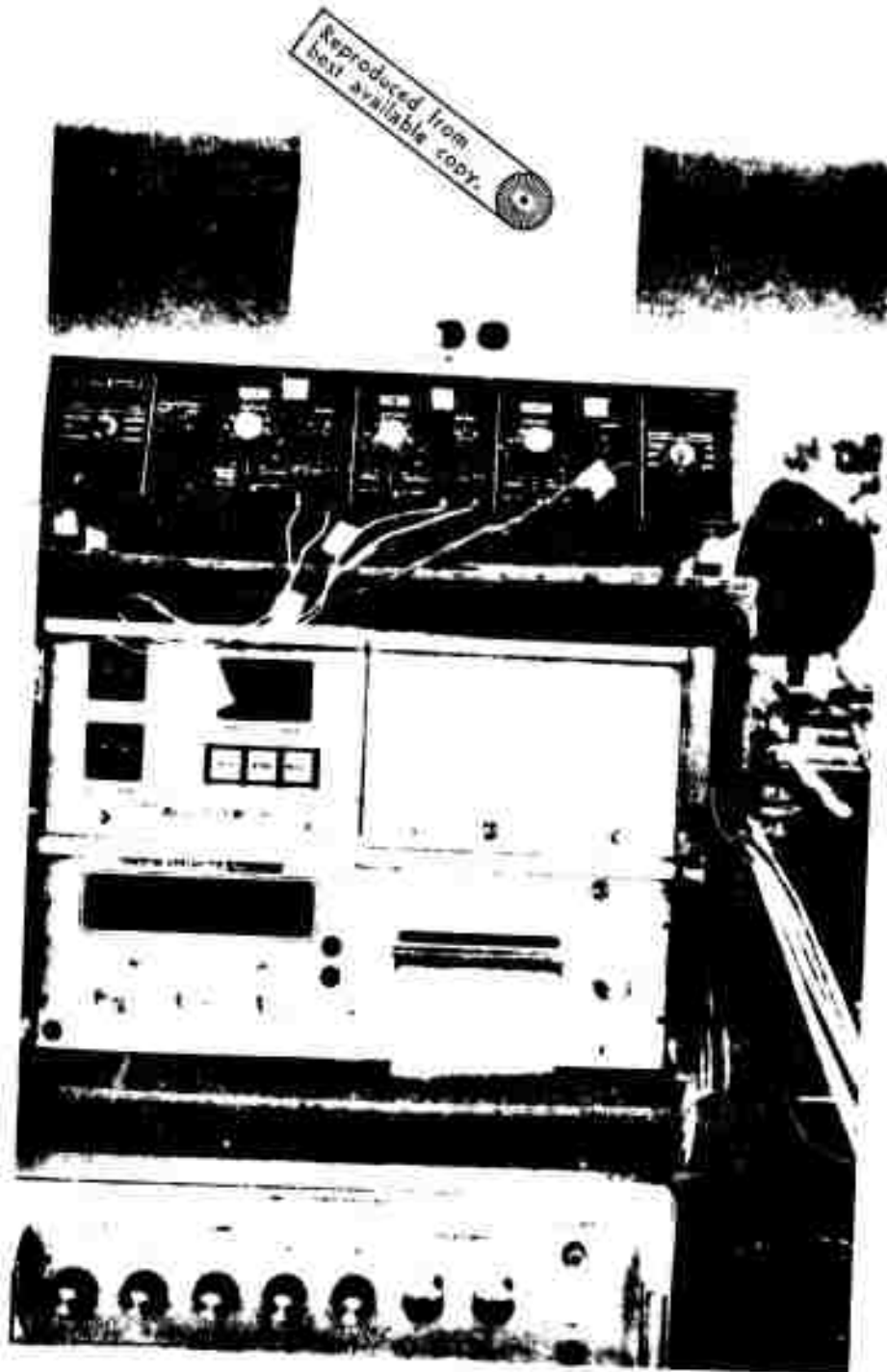
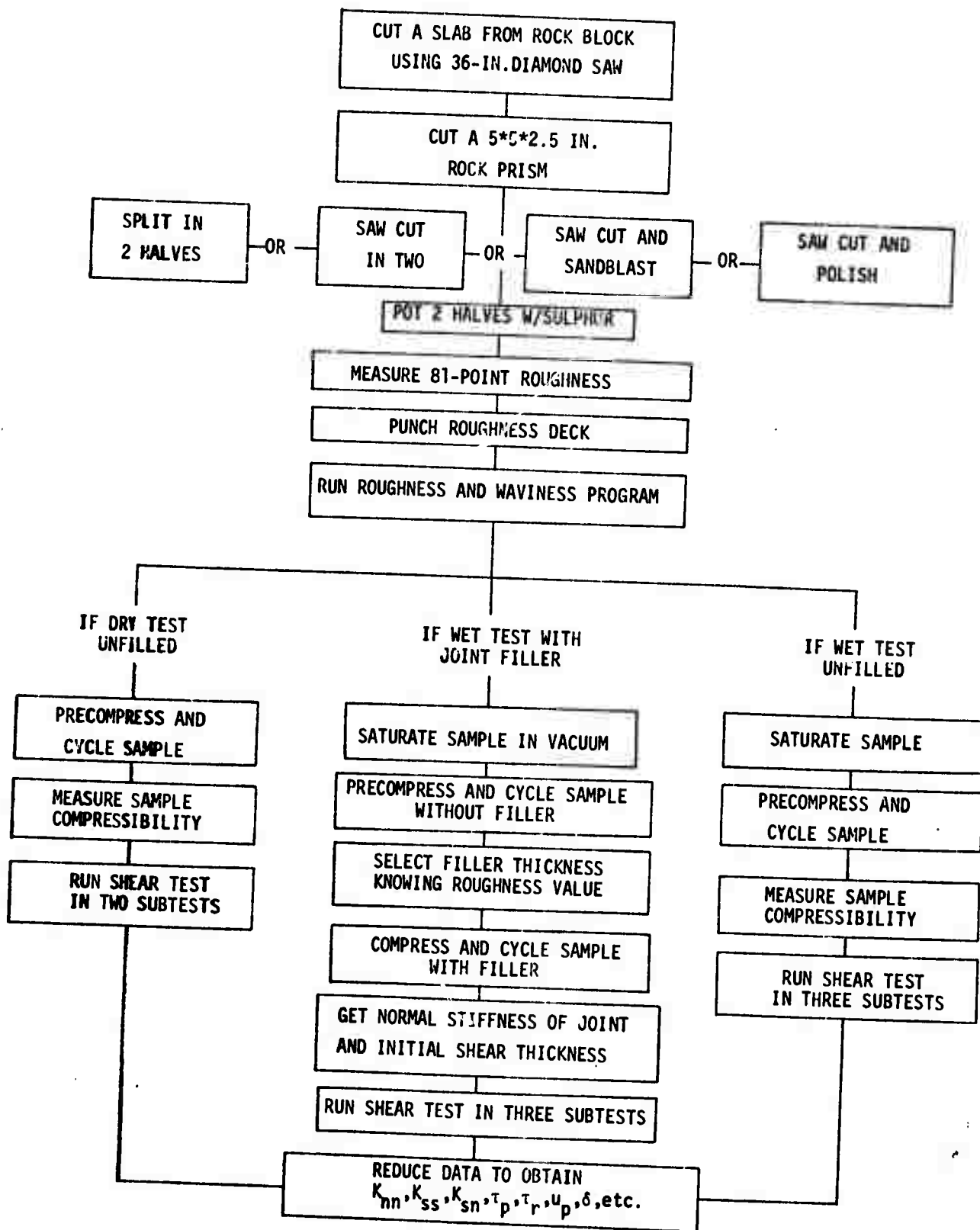


FIGURE 10: ELECTRONIC DATA RECORDING SYSTEM



OUTLINE OF TESTING PROCEDURE FOR DIRECT SHEAR TESTS

FIGURE 11

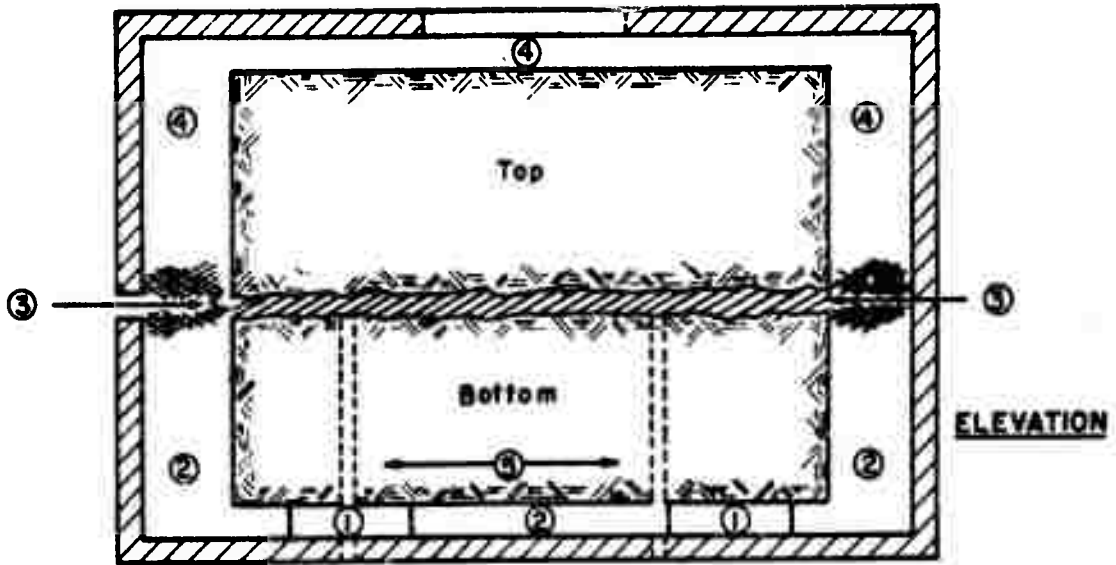


FIGURE 12 : SHEAR SPECIMEN ASSEMBLED FOR TESTING (LEGEND IN TEXT)

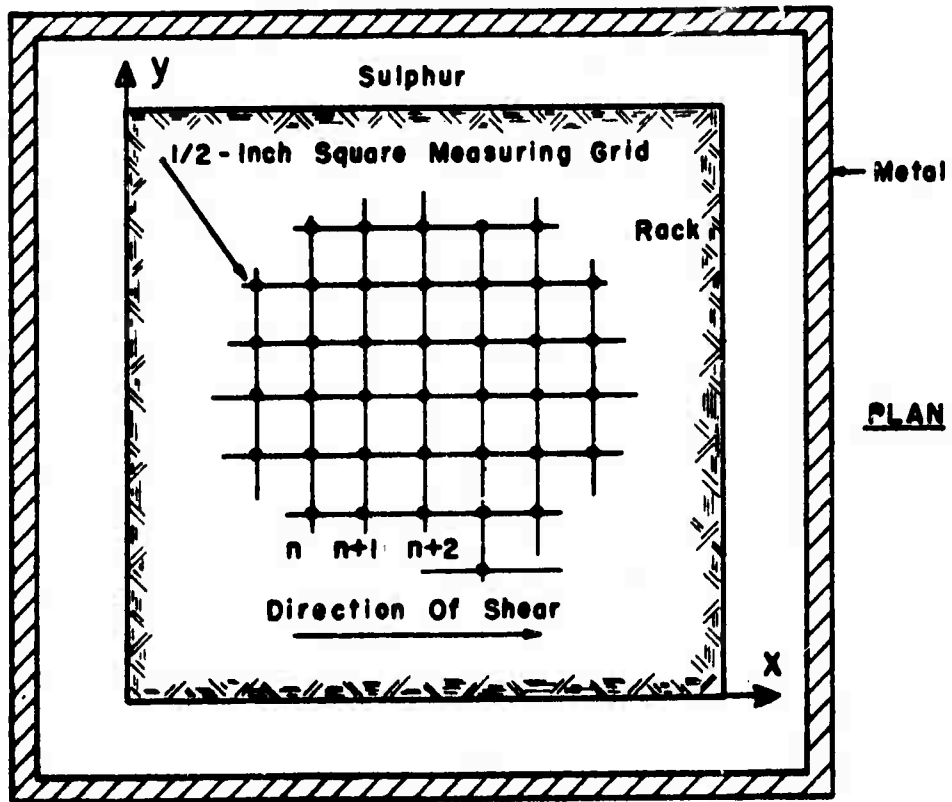


FIGURE 13 : HALF SPECIMEN LAY-OUT FOR ROUGHNESS MEASUREMENT

PART III: RESULTS OF THE TEST PROGRAM

1. PROPERTIES OF THE "GRANITE" AND THE SANDSTONE

a. Petrographic Examination

The rocks selected consist of a fine grained friable quartz arenite, and a porphyritic biotite, hornblende quartz diorite. They are described in Appendix A (prepared by Mr. Quentin Gorton).

b. Strength-Deformability and Bulk Properties

Index tests were conducted and their results are presented in table 3.

2. ROUGHNESS AND WAVINESS OF THE JOINT PLANES

a. Roughness

The values of joint roughness were presented in table 1 and are re-grouped in figures 14 and 15 where it can be seen that the various modes of preparation established distinct classes of roughness.

b. Waviness

The average slope angle is compared to the length of observation in figure 16 for various roughnesses. There is a sharp decrease in slope angle where going from 0.5 inch to a few inches. This may well indicate that at the scale of field observation the average slope angle is no more than 1 degree. Figure 17 indicates the physical relationship between measured roughness and the maximum positive slope angle. Such a relationship can probably not be applied directly to field situations considering the great difficulty in accurately describing in-situ the two parameters involved.

3. THICKNESS OF JOINT FILLER

Values for dimensionless thickness of the joint filler were presented in table 1 and are reproduced in figures 18 and 19. Without sedimentation of the clay material, it proved difficult to establish precise thickness, set

in advance. However, the measurements shown in figures 18 and 19 indicate that as for roughness, definite classes of thicknesses were established for both rock types. In this context one must remember that a value of  $T_1/R < 1$  means that the asperities of the filled joint do interlock whereas for greater values of  $T_1/R$  there is a tendency to shear through the filling material.

#### 4. DEFORMABILITY AND STRENGTH DATA

The deformability and strength values for tests on sandstone and granite joints dry and wet, filled and unfilled are presented in table 4. The order of presentation of the tests which are numbered from 1 to 72 is: sandstone dry (11), wet (13), filled (23), and granite dry (2), wet (9) and filled (14).

The following were directly measured or computed for all tests:

- peak normal stress  $\sigma_p$  maintained as close as possible to the initial normal stress value
- peak shear stress,  $\tau_p$
- ratio  $\tau_p/\sigma_p$
- residual shear stress  $\tau_r$
- shear displacement at peak,  $u_p$
- normal displacement at peak,  $v_p$
- dilatancy angle at peak  $\delta = \text{Arctan}(u_p/v_p)$ ; this angle is positive (dilation) or negative (contraction)
- shear stiffness,  $K_{ss}$  computed from the linear portion of the  $(\tau, u)$  curve.

The dilation or contraction of the joint at peak (P) and beyond is illustrated in the last column by wide or narrow signs depending upon the relative amount of dilation ( $\nearrow$ ) or contraction ( $\searrow$ ). The normal stiffness is given below for a few selected tests, following the discussion of Part II, paragraph 4 d.

Concerning values of the shear stiffness ( $K_{ss}$ ), the following must be remembered here:

1. The shear stiffness is defined as peak shear stress, to peak shear displacement ratio,

2. Accordingly a high  $K_{SS}$  can correspond to a high peak strength or a low peak displacement. So, both a strong joint with interlocking asperities, and a weak joint with very thick filler which very quickly attains its residual strength, can have high shear stiffness before their peak.

Table 5  
Normal Stiffness Values for Selected Tests on Filled Joints

Test No.	Rock Type	$K_{nn}$ ( $10^4$ psi/in)	$K_{SS}$ ( $10^4$ psi/in)	$K_{nn}/K_{SS}$	$T_1/R$	Dilatancy (o)
25	Sandstone	2.06	0.10	20.6	1.18	+ 7.5
26	"	1.99	0.71	2.8	1.32	+10.0
28	"	1.99	0.47	4.2	1.26	0
47		2.00	0.61	3.3	2.56	+ 1.8
69	Granite	1.92	0.09	22.6	1.10	+ 2.6
70	"	6.23	0.28	22.3	0.91	+ 5.5
71	"	24.9	0.30	83.0	0.54	+ 3.7
72	"	2.66	1.50	1.4	18.2	0

## 5. WATER PRESSURE DATA

The results of tests with non zero differential water pressures ( $P - p_1$  or  $P - p_2 = \Delta$ ), are presented in table 6 together with other relevant data from the tests. When discrete readings were taken during the tests, they are all given. It can be noted that both positive and negative values of the transient pore pressures were observed.

All results presented above are now discussed in Part IV.  
A typical test record is given in Appendix D (Test #61).

Table 3

Summary of Index Properties for the Rock Types of the Shear Program\*

	"Sierra White" Granite (Porphyritic Quartz Diorite)	Lyon's Sandstone (Fine Grained Quartz Sandstone)
Mineralogy	quartz 25% biotite 5% plagioclase 55% muscovite 4% K-feldspar 8% hornblende 3%	quartz 99% calcite (trace) hematite 1%
Grain size	1 to 3 mm	0.1 to 0.2 mm
Unconf. comp. strength	dry 13600 psi sat 11100 psi	4260 psi 4260 psi
E at 50% strength	dry $3.6 \times 10^6$ psi sat $3.2 \times 10^6$ psi	$0.60 \times 10^6$ psi $0.36 \times 10^6$ psi
$\nu$ at 50% strength	dry 0.25 sat -	0.30 0.26
Tensile strength	(dry) 660 psi 545 psi	260 psi 135 psi
Modulus of Rupture	(dry) 2860 psi	520 psi (fracture // to bedding)
Cohesion	(dry) 2200 psi	550 psi
Initial friction angle (dry)	54°	56°
Residual friction angle(dry)	48°	33°
Porosity	4.6%	11%
Permeability (Rw)	not measurable	3.3 millidarcys

\* Mechanical properties of the sandstone given on cores perpendicular to the bedding.

Table 4  
Strength and Deformability Data for Tests of the Shear Program

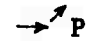
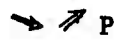


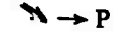


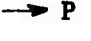





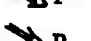




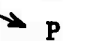
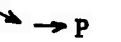





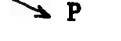
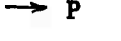
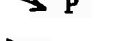
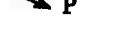

Test No.	$\sigma_p$ (psi)	$\tau_p$ (psi)	$\frac{\tau_p}{\sigma_p}$	$\tau_r$ (psi)	$\frac{\tau_p}{\tau_r}$	$u_p$ ( $10^{-2}$ in)	$\delta$ degrees	$K_{ss}$ ( $10^4$ psi/in)	Dilation at Peak
1	135	35	0.26	35	1.00	2.8	+ 2.5	0.13	 P
2	1,530	1,650	1.07	1,150	1.43	20.4	+ 0.6	0.81	 P
3	1,490	1,010	0.68	990	1.02	12.0	+ 0.4	0.84	 P
4	1,490	760	0.51	760	1.00	13.0	- 2.2	0.58	 P
5	1,500	1,000	0.67	890	1.12	11.4	- 1.6	0.88	 P
6	450	230	0.51	208	1.10	20.0	- 5.5	0.12	 P
7	500	470	0.94	440	1.07	9.6	- 0.4	0.46	 P
8	85	10	0.12	8	1.25	3.0	0	0.03	 P
9	465	230	0.50	230	1.00	5.6	0	0.45	 P
10	480	280	0.58	260	1.08	6.6	0	0.42	 P
11	108	24	0.22	24	1.00	10.0	- 3.9	0.02	 P
12	228	218	0.95	218	1.00	20.0	+ 4.4	0.14	 P
13	600	580	0.97	520	1.12	14.4	+ 0.9	0.40	 P
14	102	70	0.69	70	1.00	2.0	- 4.8	0.35	 P
15	480	420	0.88	420	1.00	14.0	- 0.2	0.30	 P
16	98	25	0.26	25	1.00	2.0	0	0.13	 P
17	500	560	1.12	545	1.02	14.0	- 1.4	0.40	 P
18	1,520	1,005	0.66	980	1.02	19.0	- 0.1	0.53	 P
19	450	275	0.61	275	1.00	16.0	- 0.4	0.17	 P
20	460	285	0.62	285	1.00	10.0	- 1.0	0.29	 P
21	1,500	1,210	0.81	975	1.24	11.0	- 0.6	1.10	 P
22	1,350	1,115	0.82	1,005	1.10	13.0	+ 0.8	0.77	 P
23	1,500	1,015	0.68	1,015	1.00	16.8	- 1.7	0.60	 P
24	1,120	710	0.63	710	1.00	16.0	- 2.0	0.44	 P
25	100	145	1.45	145	1.00	14.0	+ 7.5	0.10	 P
26	100	71	0.71	71	1.00	1.0	+ 10.0	0.71	 P
27	500	220	0.44	183	1.20	2.0	- 3.2	1.10	 P
28	100	28	0.28	23	1.22	0.6	0	0.47	 P
29	500	192	0.38	69	1.13	3.7	- 1.7	0.52	 P
30	500	261	0.52	224	1.16	2.5	- 1.2	1.04	 P

Table 4 (continued)

Test No.	$\sigma_p$ (psi)	$\tau_p$ (psi)	$\frac{\tau_p}{\sigma_p}$	$\tau_r$ (psi)	$\frac{\tau_p}{\tau_r}$	$u_p$ ( $10^{-2}$ in)	$\delta$ degrees	$K_{ss}$ ( $10^4$ psi/in)	Dilation at Peak
31	1,600	310	0.19	255	1.21	10.6	- 2.5	0.24	↘ P
32	1,310	460	0.35	375	1.22	4.5	0	1.02	→ P
33	1,510	510	0.34	485	1.05	6.6	- 0.7	0.77	↘ P
34	1,500	735	0.49	695	0.49	10.9	- 0.6	0.67	↘ → P
35	500	175	0.35	155	0.35	2.8	- 1.2	0.62	↘ P
36	500	185	0.37	170	0.37	3.7	- 1.8	0.50	↘ P
37	1,440	620	0.43	620	0.43	5.4	- 0.6	1.15	↘ → P
38	1,420	440	0.31	410	1.07	10.0	- 2.0	0.44	↘ → P
39	485	120	0.25	75	1.60	2.0	0	0.60	→ P
40	860	310	0.36	240	1.29	6.5	+ 0.5	0.48	↗ P
41	500	188	0.38	157	1.19	2.4	- 3.4	0.78	↘ → P
42	535	185	0.35	155	1.19	2.7	- 2.3	0.68	↘ P
43	500	158	0.32	100	1.58	4.5	- 0.4	0.35	↘ P
44	1,460	465	0.32	405	1.15	9.6	- 0.5	0.49	→ → P
45	1,430	460	0.32	400	1.15	6.6	- 1.0	0.70	→ → P
46	1,400	430	0.31	385	1.12	9.5	- 0.6	0.45	→ → P
47	100	98	0.98	57	1.70	1.6	+ 1.8	0.61	→ P
48	500	1,660	3.32	690	2.40	11.2	+ 11.1	1.48	↘ P
49	500	1,163	2.32	665	1.75	9.0	- 1.8	1.83	↘ P ↗
50	540	420	0.78	420	1.00	-	-	-	→ P
51	500	320	0.64	320	1.00	16.0	- 0.6	0.20	→ → P
52	640	660	1.03	505	1.30	18.0	+ 1.1	0.28	↘ → P
53	475	830	1.75	670	1.24	16.0	+ 4.0	0.52	↘ → P
54	1,570	1,100	0.77	1,100	1.00	25.0	- 0.6	0.44	P
55	1,470	975	0.66	975	1.00	20.0	- 0.2	0.49	↘ P
56	485	670	1.38	575	1.17	10.6	+ 7.1	0.63	↘ P ↗
57	1,380	1,500	1.09	922	1.63	8.8	-	1.71	↘ → ↗ ?
58	1,000	885	0.89	822	1.08	19.0	+ 4.0	0.47	↘ → ↗ P
59	505	255	0.51	255	1.00	1.4	- 14.0	1.82	↘ P ↗
60	495	140	0.28	140	1.00	0.8	- 45.0	1.75	↘ → P
61	620	540	0.87	450	1.20	10.4	- 0.6	0.52	↘ → P
62	510	480	0.94	365	1.31	5.0	+ 12.8	0.96	↘ ↗ P
63	1,470	340	0.23	340	1.00	2.4	- 1.2	1.51	↘ P

Table 4 (Continued)

Test No.	$\sigma_P$ (psi)	$\tau_P$ (psi)	$\frac{\tau_P}{\sigma_P}$	$\tau_r$ (psi)	$\frac{\tau_P}{\tau_r}$	$u_P$ ( $10^{-2}$ in)	$\delta$ degrees	$K_{ss}$ ( $10^4$ psi/in)	Dilation in Peak
64	1,480	365	0.25	290	1.26	14.6	- 3.2	0.25	⇒ P
65	624	385	0.62	346	1.11	20.0	+ 1.6	0.19	→ ↗ P
66	500	510	1.02	450	1.13	14.8	+ 4.2	0.34	→ ↗ P
67	1,440	1,345	0.93	1,170	1.15	7.2	- 0.9	1.87	→ ↘ P ↗
68	1,500	650	0.43	602	1.07	24.0	- 3.5	0.27	↘ ↗ ↘ P
69	100	120	1.20	120	1.00	13.6	+ 2.6	0.09	↗ P ↗
70	510	550	1.08	485	1.13	19.0	+ 5.5	0.28	↘ ↗ P
71	500	502	1.00	395	1.27	16.8	+ 3.7	0.30	↘ ↗ P
72	100	57	0.57	53	1.07	0.3	0	1.50	→ P

Table 6

Water Pressures Observed for Tests  
on Sandstone and Granite Joints

Test No.	$\Delta U$ Observed (psi)	Back Pressure (psi)	Roughness ( $10^{-3}$ in)	Shear Rate	$T_1/R$
19	-0.25	200	6.5	1	0
22	-4.0	600	1.8	1	0
24	-2.7	200	18.0	1	0
25	+0.3	0	75.2	1	1.2
	+0.3				
	+0.3				
26	-0.2	400	56.0	1	1.32
27	+1.6	200	10.2	1	1.66
	+1.0				
28	-0.1				
	-0.1	400	7.9	1	1.3
29	+5.0	200	8.4	2	0.10
	+5.0				
30	-3.1	400	7.3	2	0.05
	-3.7				
32	-0.8	400	7.9	1	5.6
33	+5.5	200	17.4	2	1.8
34	+4.9	400	41.8	1	0.31
35	-1.7	0	32.1	1	2.12
36	+9.9	400	41.1	1	1.90
37	-1.2	0	50.7	1	0.73
38	+0.9	400	9.9	2	0.4
39	-0.5	0	8.1	1	2.5
40	-0.5	0	8.1	1	4.7
41	+0.3	200	12.6	1	2.4
	+0.4				
42	-0.3	200	8.9	2	2.9
43	+3.2	400	9.8	2	2.7
44	-0.2	200	6.6	1	7.8
46	+0.8	400	8.7	2	8.9

Table 6 (continued)

Test No.	$\Delta U$ Observed (psi)	Back Pressure (psi)	Roughness ( $10^{-3}$ in)	Shear Rate	$T_1/R$
47	-1.1	0	8.2	1	2.6
51	-0.25	600	1.9	1	0
52	-0.20	200	67.2	1	0
54	+2.8	200	0.9	1	0
60	+0.7	600	1.1	1	42.8
	-1.4				
61	+25.2	200	51.6	1	1.4
	+22.6				
62	+0.6	400	117.5	1	0.43
	-5.7				
	+0.7				
	+0.6				
	+7.3				
65	-0.1	400	50.5	2	0.91
	-0.3				
	-0.2				
66	+0.2	400	66.4	1	1.10
	-0.3				
67	+1.8	200	66.2	1	0.31
68	+7.5	400	63.5	1	0.36
69	+0.6	400	52.5	1	1.10
	+1.4				
	+2.2				
70	+2.6	400	59.4	2	0.91
71	+5.4				
	-0.3	0	59.4	1	0.54
72	+0.4	400	2.3	1	18.2
	-0.1				

Table 7  
Influence of the Test Program Variables  
on Joint Deformability Parameters

Variation  $\partial X/\partial Y$ : Sandstone

X	Y				
	$\sigma_n$	R	$T_1/R$	t	$P_b$
$K_{ss}$	dry, wet: >0 filled : ?	dry, wet >0 for R>25	>0 ? for $T_1/R > 10$	slightly <0	wet tests: >0 filled : ?
$u_p$	>0	dry: slightly >0 wet: $\approx 0$ except >0 for $\sigma_n < 100$	$\approx 0$	slightly >0?	slightly >0?
$\delta$	<0 counteract each other	>0	$\approx 0$ $T_1/R < 20$ slightly >0 for $T_1/R > 20$	-	-

Variation  $\partial X/\partial Y$ : Granite

X	Y				
	$\sigma_n$	R	$T_1/R$	t	$P_b$
$K_{ss}$	wet >0	>0 when $R > 70 \times 10^{-3}$	>0	inconclusive	wet : >0 filled: $\approx 0$
$u_p$	>0	Apparently <0	inconclu- sive	inconclusive	apparently <0
$\delta$	wet: >0? at $\sigma_n < 1,500$ filled: <0	>0	-	-	-

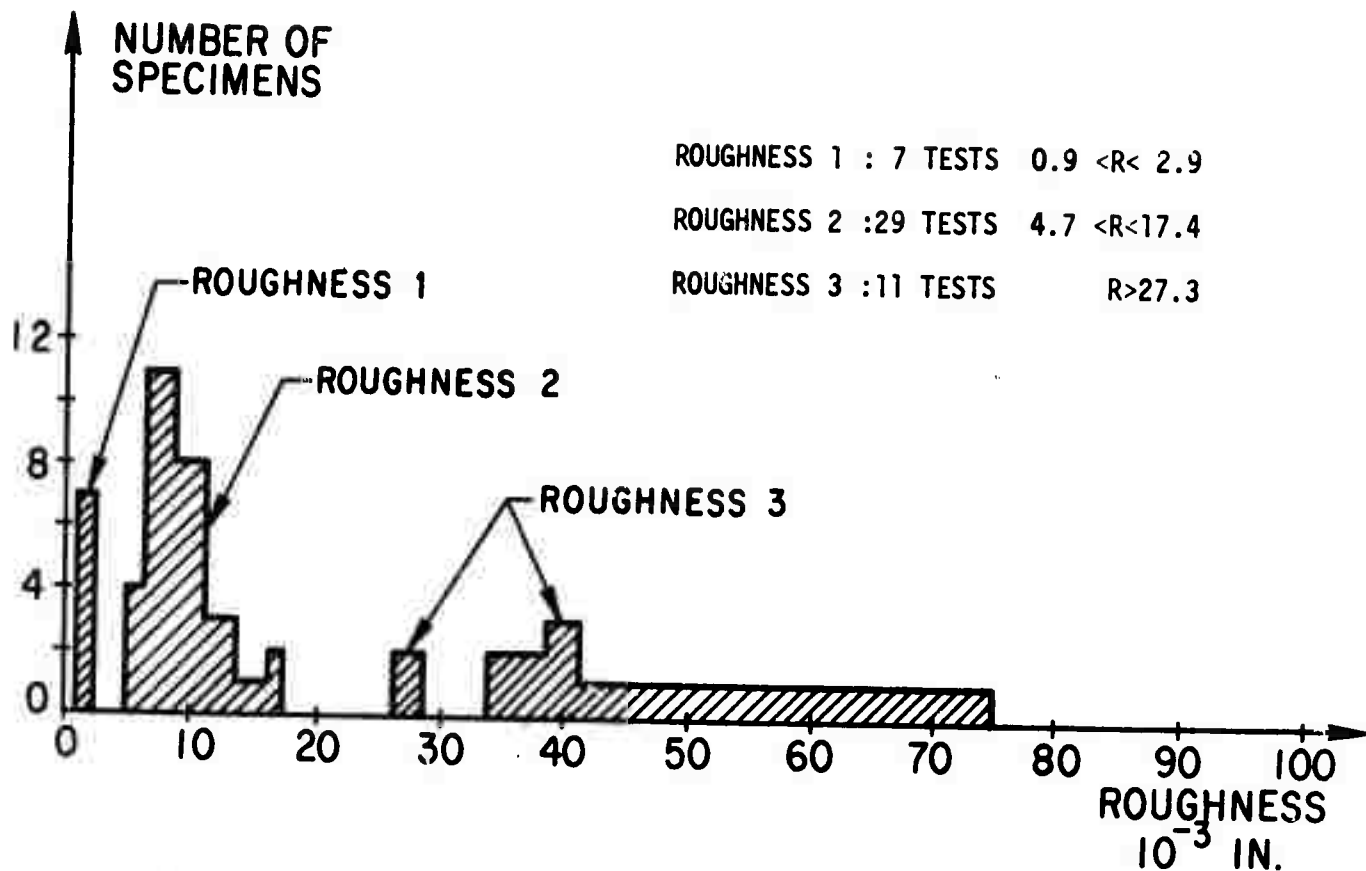


FIGURE 14 : ROUGHNESS DISTRIBUTION OF SANDSTONE JOINTS

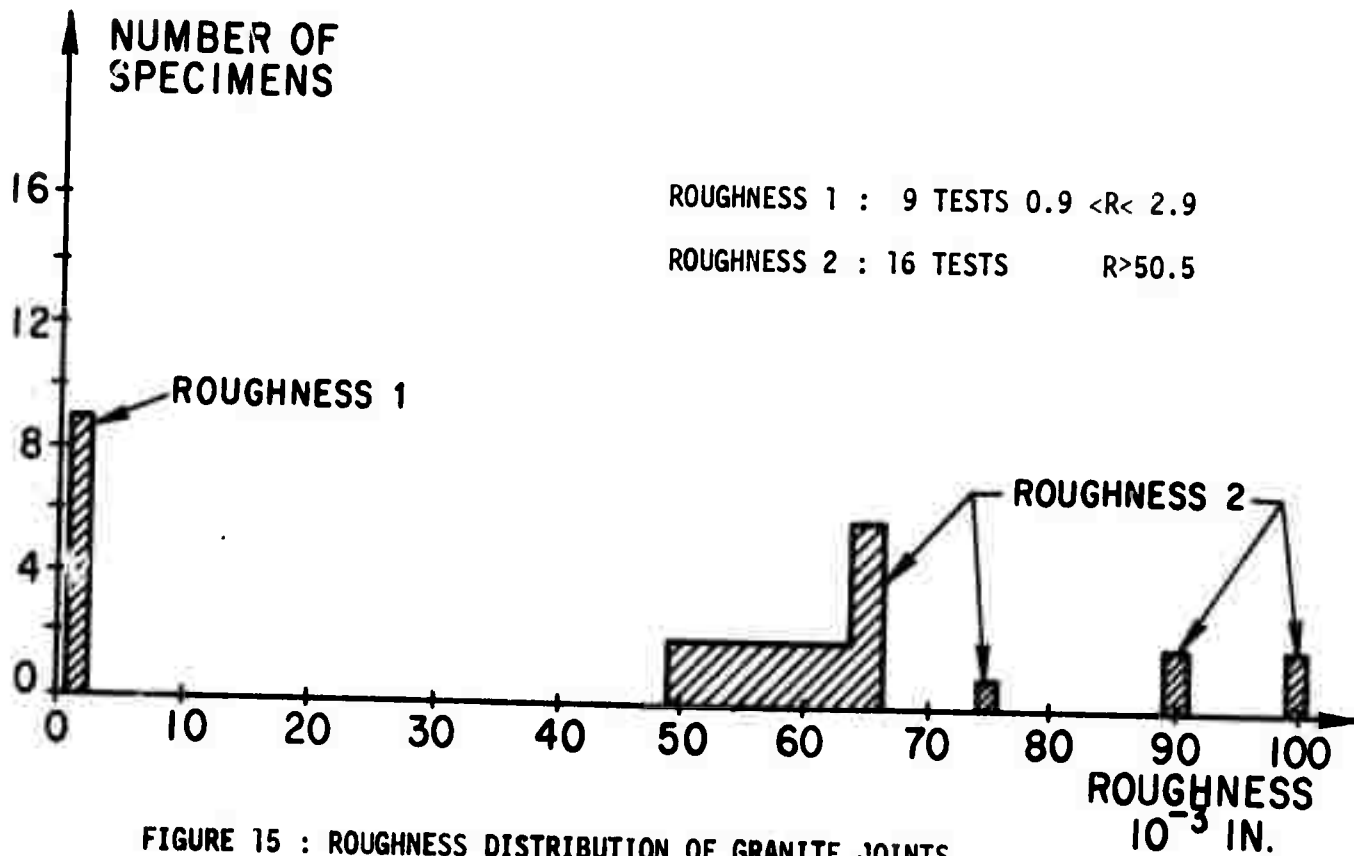


FIGURE 15 : ROUGHNESS DISTRIBUTION OF GRANITE JOINTS

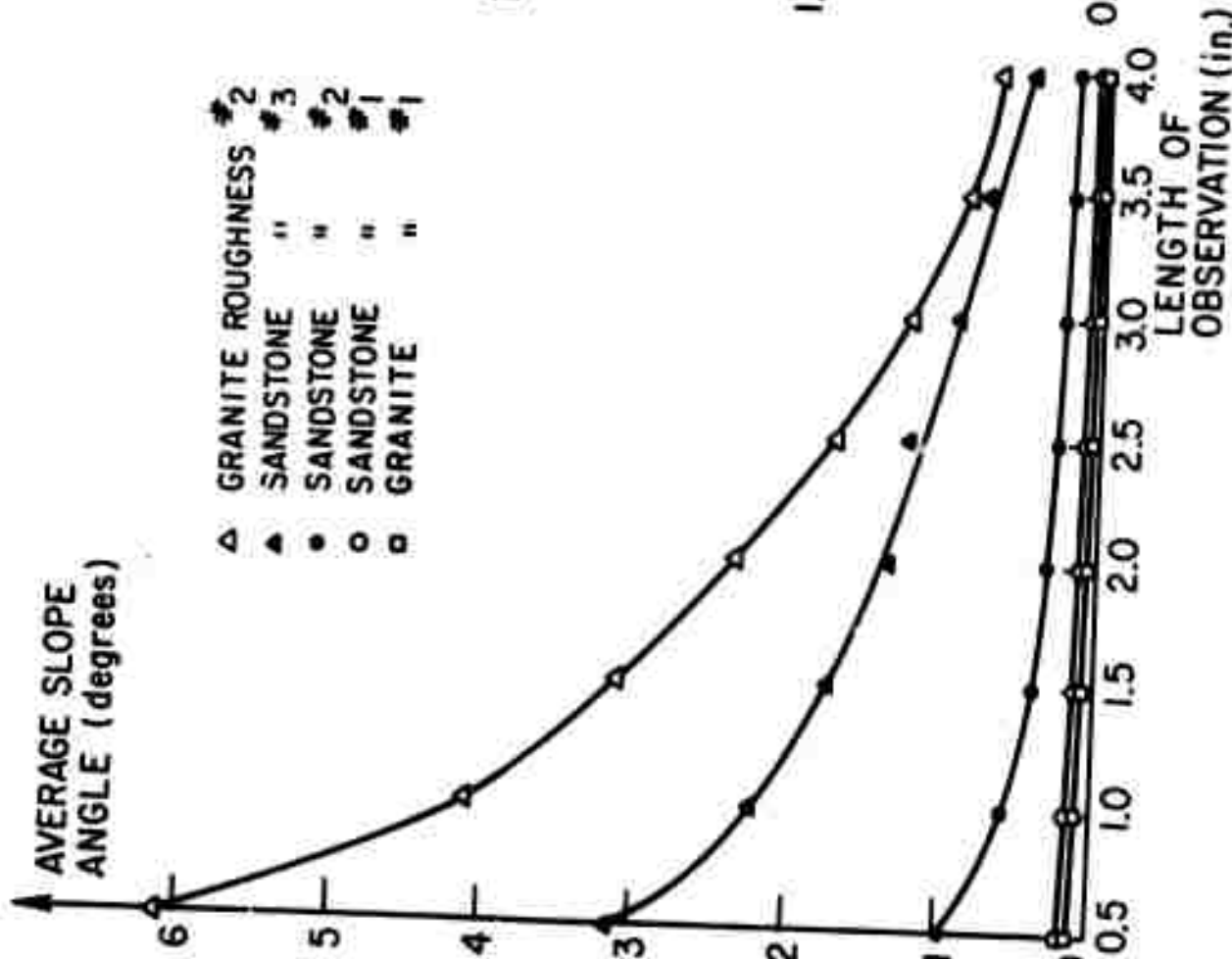


FIGURE 16

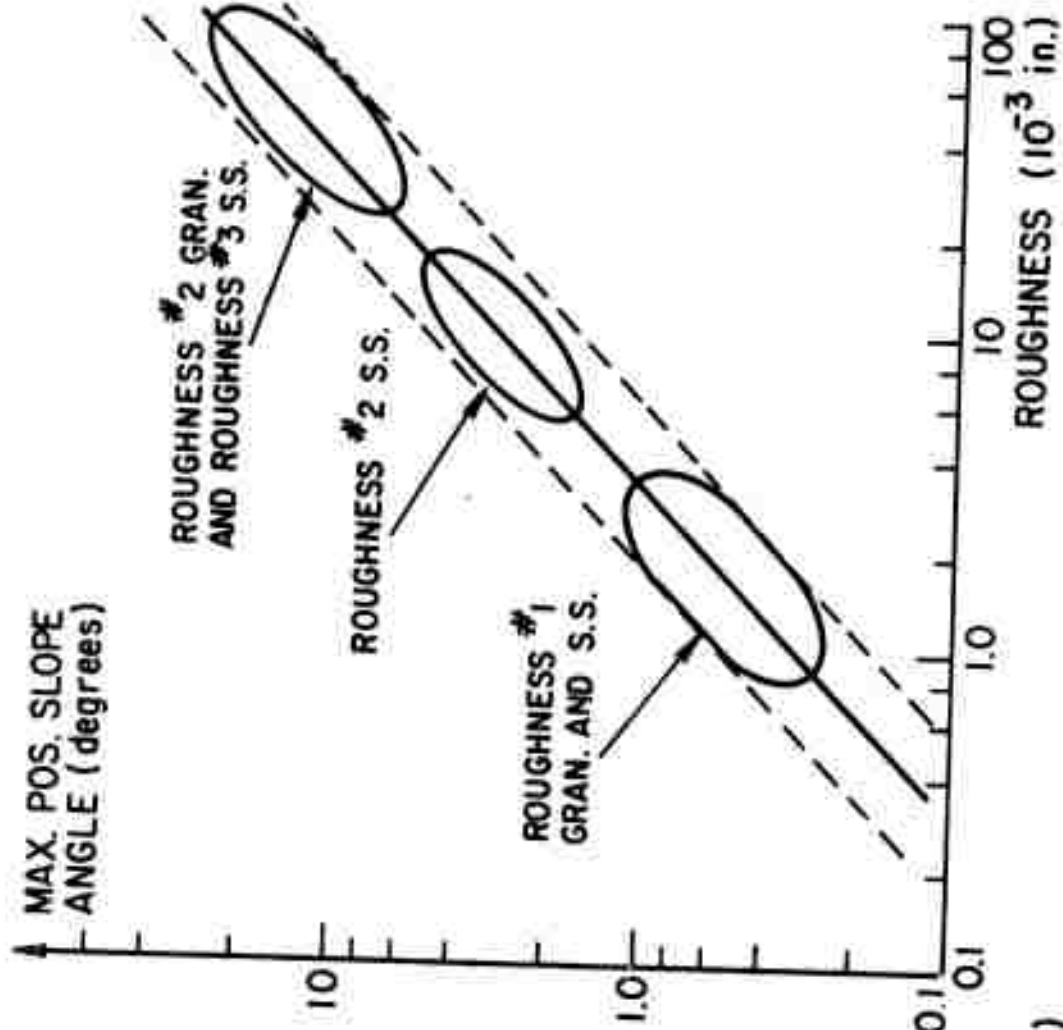


FIGURE 17

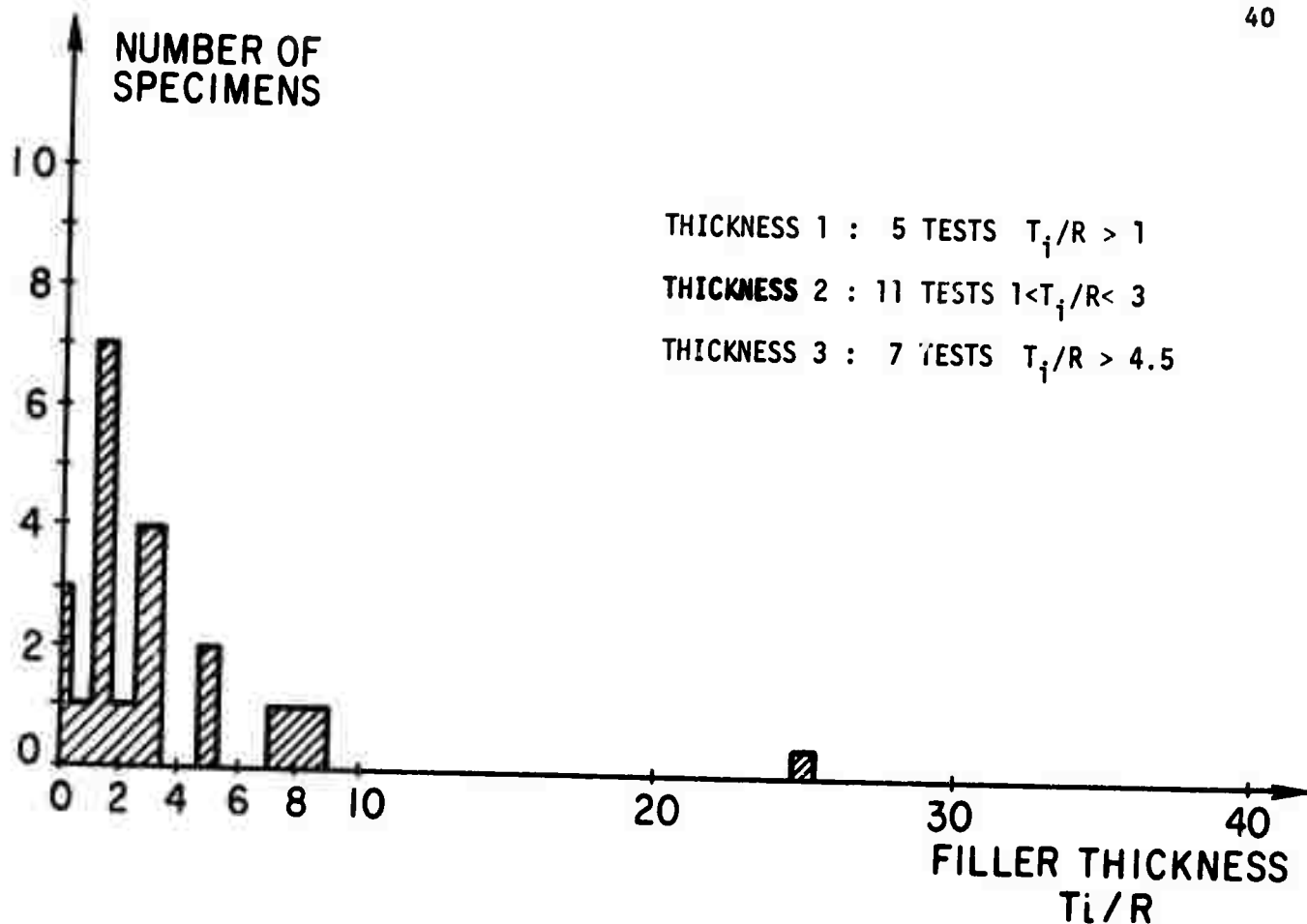


FIGURE 18 : DIMENSIONLESS FILLER THICKNESS ( $T_i/R$ ) FOR SANDSTONE JOINTS

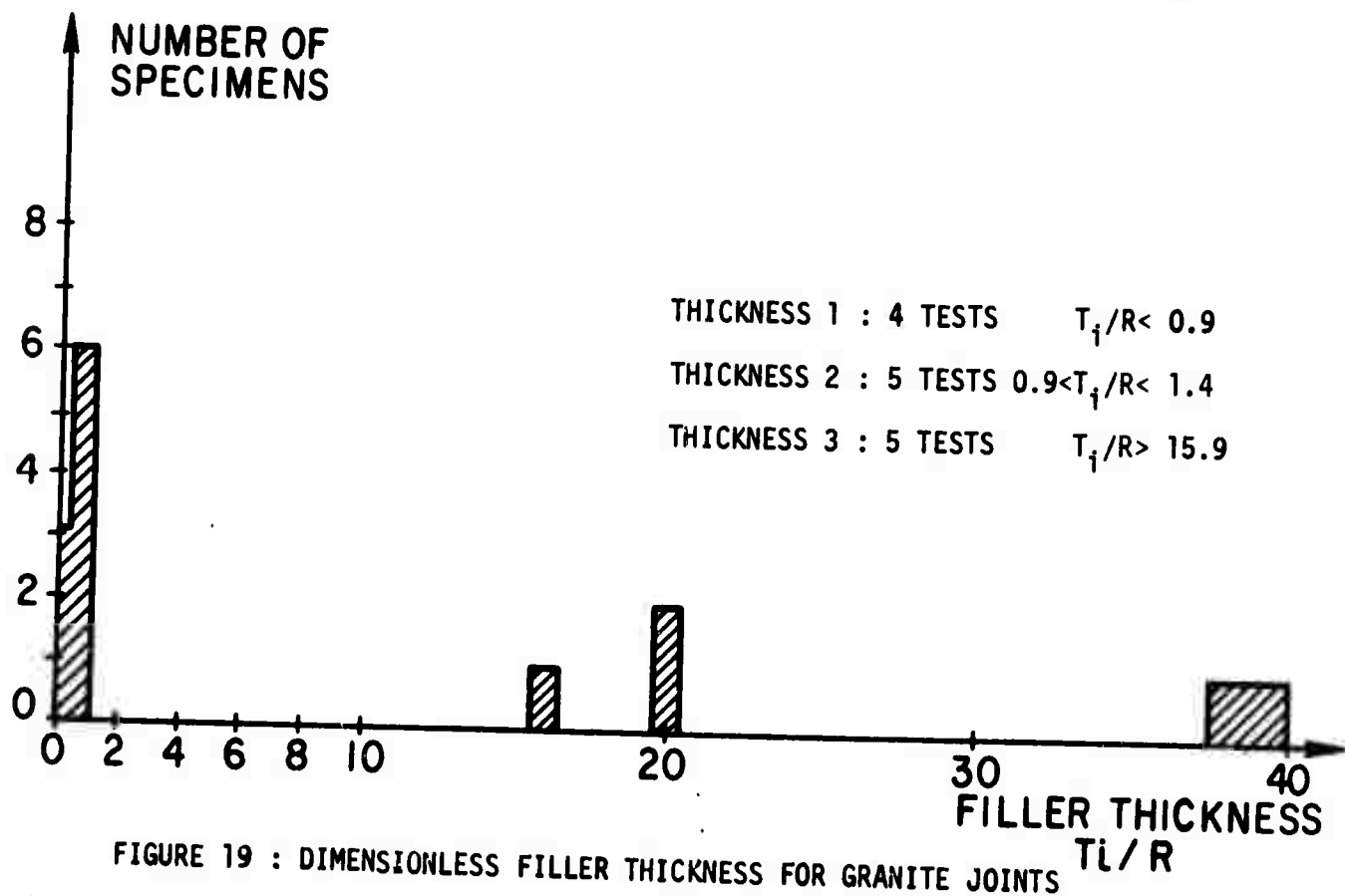


FIGURE 19 : DIMENSIONLESS FILLER THICKNESS FOR GRANITE JOINTS

## PART IV: DISCUSSION OF THE TEST RESULTS

The three groups of properties subject to discussion are: 1) the deformability parameters:  $K_{ss}$ ,  $u_p$  and  $\delta$ , 2) the strength parameters:  $\tau_p$ ,  $\tau_r$  and 3) the water pressures  $P$ ,  $p_1$ ,  $p_2$ . The values observed are analyzed in terms of their variation as a function of the variables in the testing program, namely:

The normal pressure,  $\sigma_n$ .

The joint filler thickness,  $T_f$  or  $T_f/R$ .

The shear rate,  $\dot{\tau}$ .

The back pressure,  $P$ .

The roughness,  $R$ .

### 1. DISCUSSION OF JOINT DEFORMABILITY

#### a. Sandstone Joints

##### Shear stiffness: $K_{ss}$

- increases with increasing  $\sigma_n$  for dry and wet tests
- no pattern for filled tests
- fairly insensitive to  $T_f/R$  except at high values (say  $>10$ )
- appears to decrease when shear rate  $\dot{\tau}$  increases
- fairly insensitive to  $R$  in dry and wet tests except at high values say  $R > 25 \cdot 10^{-3}$
- appears to increase with increasing  $P_b$  in non-filled tests. Not conclusive for filled joints.

##### Shear displacement at peak: $u_p$

- increases with  $\sigma_n$  in all tests (ploughing). The effect is less felt on filled joints, and the absolute value of  $u_p$  is smaller with filled joints.
- increases slightly with increasing roughness (dry tests)
- the travel to  $u_p$  amounts to several times the roughness. Many

asperities must be sheared before reaching the peak.

- in wet tests  $u_p$  is almost independent of  $R$  except at low pressures ( $\approx 100$  psi).
- insensitive to  $T_1/R$  ( $T_1/R$  was  $< 18$ )
- may increase slightly with higher shear rate
- may increase slightly with higher  $P_b$

$\sigma_n$  overshadows every other parameter for influence on  $u_p$ .

Dilatancy angle:  $\delta$

Roughness 3 is not a natural roughness. It will give a contraction in most cases ( $\delta < 0$ ). Eliminating tests with roughness 3 it appears that even at high values of  $R$  (up to  $45 \times 10^{-3}$ ),  $\delta$  stays small in this weak rock ( $< 4^\circ$ ) (dry tests). In wet tests, and for roughness 4 there is a strong decrease of  $\delta$  with  $\sigma_n$ . For wet or filled tests the no-dilatation pressure is below 500 psi, whatever the roughness. For filled joints it takes a very large  $T_1/R$  ( $> 20$ ) to influence  $\delta$ . The primary factor is  $R$ .

#### b. Granite Joints

Shear stiffness:  $K_{ss}$

- increases with  $\sigma_n$  in wet tests
- effect of  $R$  is not conclusive except at high values ( $R > 70 \times 10^{-3}$ ) where  $K_{ss}$  increases  $T_1/R$ . This increase in  $K_{ss}$  can be accompanied by lower strength; joints with high  $T_1/R$  can have high  $K_{ss}$  and low strength.
- effect of  $\dot{\tau}$  is not conclusive
- in wet tests  $K_{ss}$  seems to increase markedly with higher  $P_b$
- this is not exhibited in filled tests.

Shear displacement at peak:  $u_p$

- increases with higher  $\sigma_n$  (wet tests)
- seems to decrease when  $R$  increases
- the values of  $u_p$  are comparable to those for sandstone everything else

being equal

- results of filled tests are not conclusive here, for the influence of  $\sigma_n$  or  $T_1/R$ , or  $P_b$
- results are not conclusive for the influence of  $\dot{\tau}$
- $u_p$  would seem to become smaller when  $P_b$  increases; under higher  $P_b$  the peak is reached sooner (in wet tests).

Dilatancy angle:  $\delta$

Wet tests:

- the primary factor is again R
- below  $\sigma_n = 1,500$  psi and for large roughnesses,  $\delta$  is not sensitive to  $\sigma_n$
- the no-dilatancy pressure is in excess of 1,500 psi

Filled tests:

- filled joints do not dilate at  $\sigma_n = 1,500$  psi, irrespective of joint roughness.

For the reader's convenience the previous conclusions are condensed in table 7.

## 2. DISCUSSION OF JOINT STRENGTH

The strength of the joint specimens will be discussed with reference to points plotted in the  $(\tau, \sigma)$  plane. Figure 20 shows peak shear stress ( $\tau_p$ ) versus  $\sigma$  for all tests with dry and wet sandstone while figure 21 shows residual strength  $\tau_r$  versus  $\sigma$  for the same tests. The roughness, in  $10^{-3}$  inches, is given beside each  $(\tau, \sigma)$  point. Lines at  $28^\circ$ ,  $34^\circ$ , and  $43^\circ$  from the origin have been shown as guides for reference. There is considerable scatter about these lines. The following comments derive from figures 20 and 21. Peak and residual strengths are about the same for the sandstone. The sandblasted specimens (roughness 2) show the lowest strengths of the three roughness groups; this method of rough joint production is unsatisfactory for unfilled joints as the halves of the specimen do not mate. Water raises

the strength slightly. Whether this is a true antilubrication effect or an apparent effect contained within the scatter band is not definite.

The roughest specimens, produced by splitting (roughness 3), display evidence of a downward bend in the strength curve; a bend is shown at  $\sigma_p$  equal to about 600 psi. However the data are insufficient to definitively compare confidence limits for straight versus curved strength lines. The saw cut surfaces always give  $\phi = 34^\circ$  which can therefore be accepted as the friction angle ( $\phi_\mu$ ) for the sandstone.

Peak and residual shear strength data for tests with wet, unfilled joints in granite are given in figures 22 and 23 respectively. There is little difference between peak and residual strength for the specimens with slight roughness produced by diamond sawing; the friction angle  $\phi_\mu$  equals  $35^\circ$ . The rough specimens produced by splitting have peak and residual strengths considerably stronger by virtue of geometric effects.

Figure 24 presents strength data for tests on clay-filled joints in granite and sandstone. The strength curve for filling material alone is shown by the dashed line; it was derived from tests with a large ratio of clay thickness to joint roughness ( $T_1/R$ ). The tests with very thin filling show augmented strength by virtue of the geometric affect of the rough walls. As its thickness is increased, clay filling reduces this strength to that of filling material alone. The wall rock ceases to exert an influence on the joint strength when ( $T_1/R$ ) becomes greater than about 3. Because of scatter in results, attempts to quantify the results further would be ill-founded until more are obtained. It is important to note, however, that the gouge effect on strength revealed by these data is very significant, as it changes rock mass strength by as much as a factor of 4.

### 3. DISCUSSION OF WATER PRESSURE RESULTS

In a program of direct shear tests on marl-filled seams, Coyne and Bellier experienced difficulty in obtaining a uniform degree of saturation if the field moisture content was not preserved. With this in mind we designed a system to apply back pressure to theunjacketed specimens; any variability in results deriving from incomplete saturation could then be removed by raising the back pressure sufficiently high. The system can hold up to 700 psi chamber pressure. That the results showed insensitivity to back pressure level demonstrates that complete saturation was not elusive in this program.

The more significant water pressure variable investigated is the joint water pressure induced during shearing without drainage. During a test of a rough joint at low confining pressure, dilation generally occurs. The increasing volume of the dilating joint would be responded by water flow from the chamber into the joint; since flow is retarded by the restricted joint permeability, a negative water pressure transient should develop. Converseley, under high normal pressure where contractancy occurs, a transient water pressure increase should occur. Since the specimens were not jacketed the full pressure buildup would not be measured unless very rapid loading were obtained - i.e. peak loading in a time increment smaller than the time for a pressure pulse to transit the specimen. In this program, such loading rates were not attained and large pressure buildups were not measured. However the sign of induced water pressures consistently followed the above geometric effects, as shown by a comparison of table 6 (column 2) and table 4 (extreme right column). Dilating specimens showed pore pressure decrease of up to 6 psi. Contracting specimens show pore pressure buildup of up to 25 psi. As noted earlier, these pressure indications may be less than the actual pressure peaks in the joint; only two places in the joint were sampled by the piezometers. In the tests currently underway with jacketed specimens, larger pressures are

being observed.

Superimposed on the geometric effect described above one can expect a particle rearrangement effect in the clay of the filler material. Since remoulded clay filler was used, pore pressure buildup from this source was not found. Tests with a filler which undergoes structural collapse on shearing, such as porous plaster and preconsolidated clay are planned in the continuation of this program.



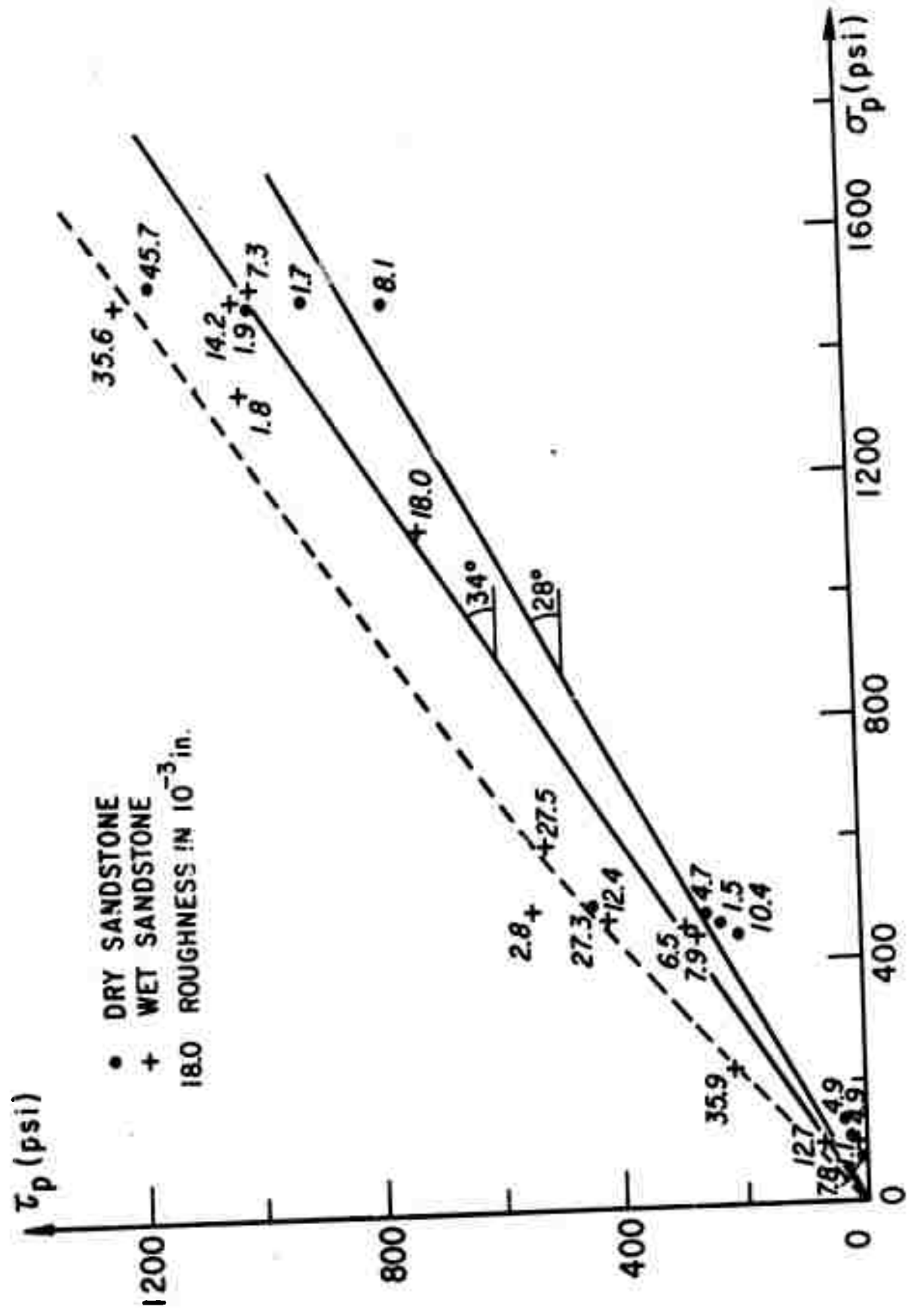


FIGURE 21 : RESIDUAL STRENGTH OF SANDSTONE SPECIMENS

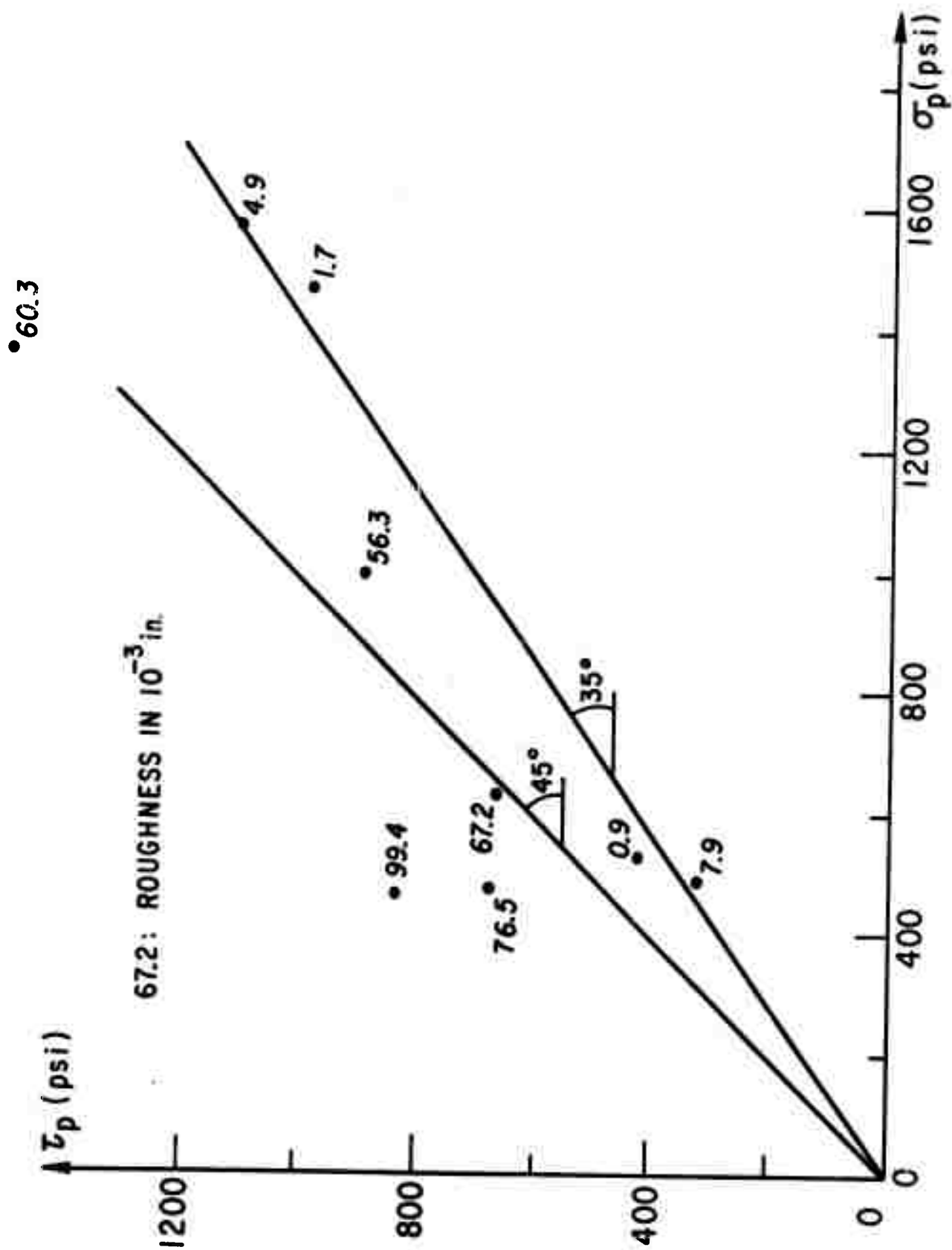


FIGURE 22 : PEAK STRENGTH OF WET GRANITE SPECIMENS

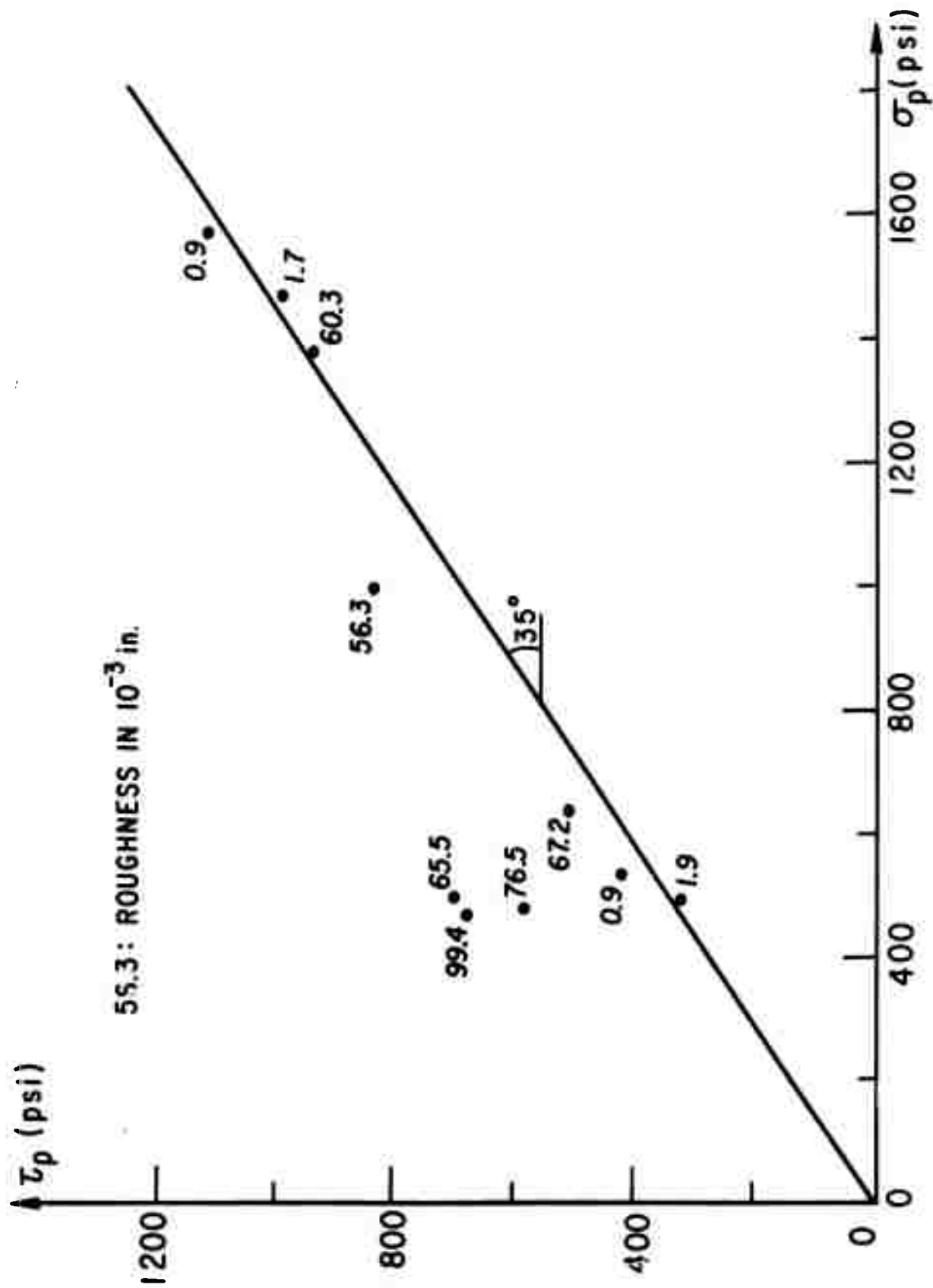


FIGURE 23 : RESIDUAL STRENGTH OF WET GRANITE

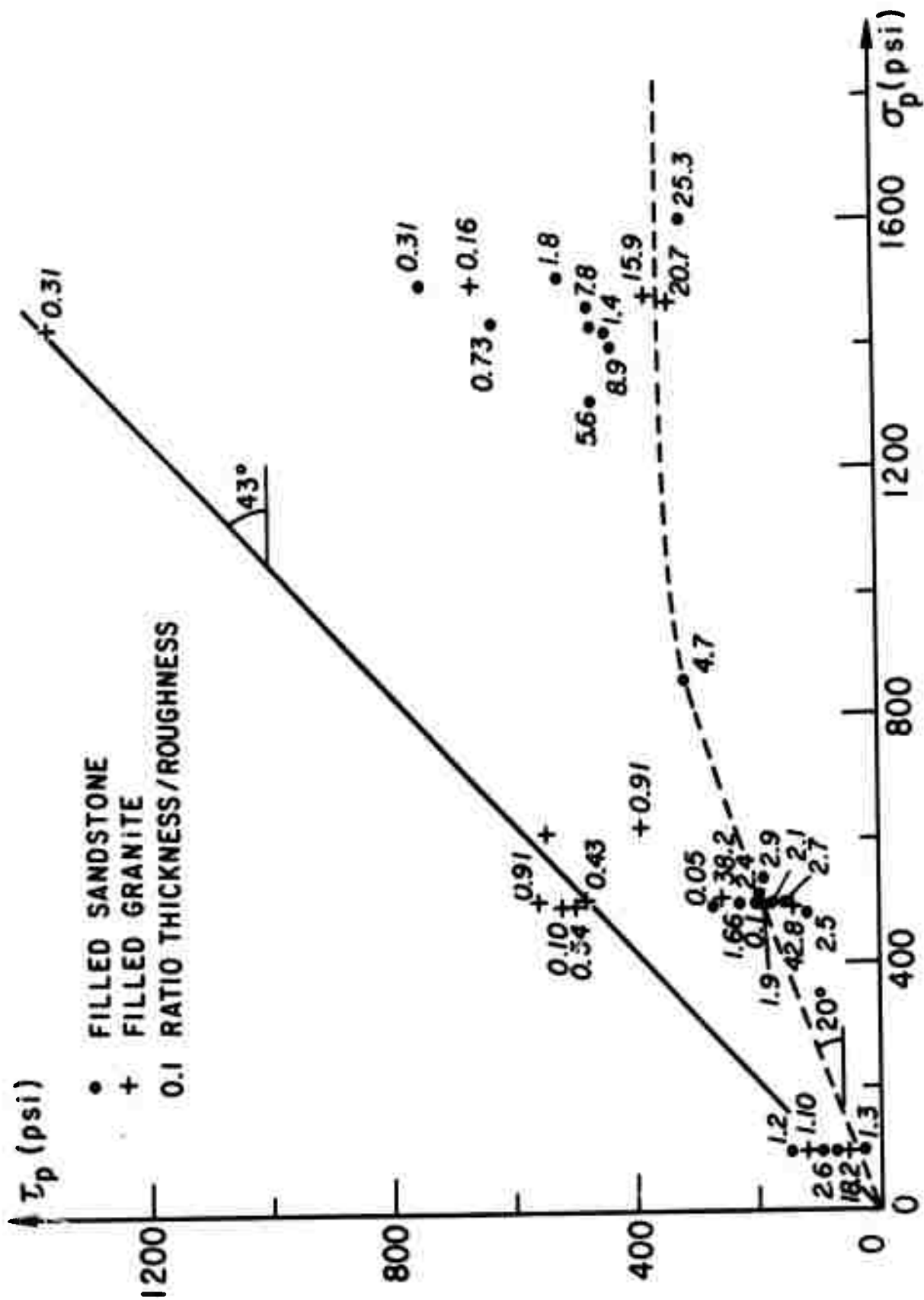


FIGURE 24: STRENGTH DATA FOR CLAY FILLED JOINTS

PART V: SUMMARY-CONCLUSIONS

A program of direct shear tests on samples of rock joints was initiated to gain an improved picture of the deformation and strength of jointed rock masses under load. The shear testing machine, developed under an NSF grant, and improved during this project, allows water pressure to be monitored in the joint plane during shearing. Seventy-two tests were conducted in this first year of an intended 3 year's program; artificial joints were created in two rock types -- granite and sandstone -- with varying wall roughness, filling material thickness, and environmental conditions.

The methods of preparing joint specimens of varying roughness were developed in this project; rough artificial joints were manufactured by splitting the specimens and smooth joints by diamond sawing and lapping. It was difficult to fill the joints to a predetermined thickness with gouge preconsolidated to a desired high normal pressure; remoulded gouge was therefore introduced. Roughness measurements were made and statistical parameters of roughness and waviness were computed using two specially written programs to be found in Appendices B and C. Typical test records are also given in the Appendix.

Table 7 summarizes the sensitivity of deformability and strength parameters to the variables studied. For the sandstone and granite specimens, both peak displacement and joint stiffness varied with normal pressure. The dilation angle decreased rapidly with normal pressure for both rock types and became negative for the sandstone specimens at  $\sigma$  above 500 psi (i.e. the specimens contracted during shear). Induced water pressures measured were not large ( $<25$  psi), possibly due to the problem of sampling water pressures in the joint plane, partly due to the remoulded nature of the filling, and partly because of decay of the water pressure transients in the unjacketed specimens. Dilatant joints generally suffered an increase in pressure while contractant joints underwent a pore pressure buildup. Complete saturation of the joints was obtained, as

evidenced by the insensitivity of the results to chamber back pressure. Filled joints approached the strength of the clay filling material when the thickness was greater than about 3 times the mean roughness amplitude.

Joints and faults exert controls on rock movement below ground and their weakness and deformability limit the "hardness" of underground sites. Furthermore, water pressure phenomena create difficulties for design and construction. This research has added to the technology basis to rational engineering with rock masses. In the work, basic phenomena of jointed rock are being examined experimentally for the first time permitting formulation of correct constitutive laws for joints that are vital to numerical and physical modelling. In continuation, tests with jacketed specimens having preconsolidated filler material are proposed. Experimental methods for these improvements in testing technique have now been developed.

REFERENCES

1. Coulson, J. H. (1970) "The Effect of Surface Roughness on the Shear Strength of Joints in Rocks", Technical Report MRD-270 to U.S. Army Corps of Engineers, Omaha, Nebraska by Dept. of Civil Eng., Univ. of Illinois, Urbana.
2. Fecker, E. and Rengers, N. (1971) "Measurement of Large Scale Roughnesses of Rock Planes by Means of Profilograph and Geological Compass", Proc. Symposium Int. Soc. Rock Mech., Nancy, France, October.
3. Goodman, R. E. (1970) "The Deformability of Joints" in Determination of the In-Situ Modulus of Deformation of Rock, ASTM, Special Techn. Publ. 477, pp. 174-196.
4. Houston, W. N. (1967) "Properties of Kaolinite Clay", Appendix to Ph.D. Dissertation, Geotechnical Engineering, Univ. of California, Berkeley.
5. Kutter, H. K. (1971) "Stress Distribution in Direct Shear Test Samples", Proc. Symposium Int. Soc. Rock Mech., Nancy, France, October.

APPENDIX A

PETROGRAPHY AND MINERALOGY OF THE PROJECT'S ROCK TYPES

( Q. GORTON )

## 1. PETROGRAPHY OF IMPERVIOUS ROCK SAMPLE

### a. Description of Specimen

A block specimen was purchased from a dimension stone quarry near Rocklin, California located on the western flank of the Sierra-Nevada batholith. These mesozoic granitic intrusives range in composition from granite (var. Alaskite) to quartz diorite (tonalite), with quartz monzonite (adamellite) and granodiorite being the most prominent rock types. The quarry is operated within an intrusive body several square miles in extent and mapped as quartz diorite and diorite.

The block specimen appeared sound and unweathered, as judged by fracture through constituent grains on broken surfaces and lack of any discoloration often associated with weathering. It also appeared to be typically isotropic except for the presence of quartz veinlets which traversed the rock in a random fashion at intervals of about one foot. These veinlets, ranging in thickness from .5 to about 2.0 mm, consisted principally of clear quartz with accessory amounts of pyrite. Careful inspection of the rock surface and past experience with such phenomena indicate that the mechanical isotropy is not affected by these apparent discontinuities.

Petrographic examination of the rock both in hand specimen and thin section showed it to be holocrystalline, phaneritic with hypidiomorphic-granular texture.

### b. Mineralogical composition

#### Essential minerals

quartz	clear and unaltered	25%
plagioclase (var. oligoclase)	frequent albite twinning with numerous, narrow lamellae; zoning is apparent from optical characteristics, and selective alteration of calcic rich zones was noted, but the type of zoning (normal, reverse, or oscillatory) was not positively determined.	55%

## Accessory minerals

K-feldspar	some Carlsbad twinning present; no zoning observed, but grains were moderately altered, as determined by the degree of pitting.	8%
biotite	pleochroic-yellowish brown to brown	5%
muscovite	non-pleochroic, colorless	4%
hornblende	pleochroic-pale green to green	3%

### c. Grain Fabric

The accessory minerals and plagioclase appeared as grains measuring 1 to 3 mm. While the quartz was also represented in this size range, several individuals had dimensions of 10 to 12 mm. Therefore, the rock could be considered as having a poorly developed porphyritic texture, which is significant in that rocks of this composition seldom occur as bonafide porphyries. The rock can be called porphyritic biotite-hornblende quartz diorite (tonalite).

## 2. PETROGRAPHY OF PERVIOUS ROCK SAMPLE

### a. Description of Specimen

A block specimen was purchased from a demolition company in Denver, Colorado, after serving as a large building stone for about a century. The building was typical of those in the old section of Denver, being constructed of red colored dimension stone quarried from the Lyons Sandstone formation. The Lyons Sandstone is a member of the Permian Cassa group and measures 50 to 200 feet thick in its domain of central northern Colorado. The block specimen appeared deteriorated an inch or less from the surface, the remainder being uniformly soft and friable. However, without comparing this sample with the equivalent in-situ formation, it is difficult to determine if the rock is characteristically poorly indurated, or if it has been severely weathered by a century of atmospheric exposure. Although the sample is fairly homogeneous, traces of cross-bedding can be observed, along with less definite indications of bedding or ground water leaching and staining. Even with a block sample, these features are so large scale that they cannot be correctly interpreted without reference to the original outcrop. Preliminary work with the block specimen suggests that this slight expression of fabric does not significantly affect the mechanical isotropy or homogeneity of the rock. Petrographic examination of the rock in both hand specimen and loose grains yielded the following additional information (a thin section was attempted, but the friable nature of the rock prevented proper preparation, using simple methods):

### b. Mineralogical Composition

#### Detrital grains

quartz	clear with surface staining from hematite cement	99%
--------	--	-----

Matrix material

iron oxide (hematite)	reddish material coating loose grains, and partially filling the void space between grains	1%
calcite	may have been a co-binder at one time, as evidenced by spotty reactions to dilute acid treatment; however, it is no longer an effective cementing agent either because of in-situ leaching or atmospheric exposure.	trace

c. Grain Fabric

The detrital grains are generally equidimensional (sphericity .8 to .9). They are commonly subrounded with larger individuals rounded and smaller ones subangular (roundness .5 to .8). The grain population appears well sorted with an average size of .10 to .15 mm and a maximum size of about .20 mm. The sandstone is poorly consolidated, exhibiting tangential intergrain contacts, and demonstrates an open pore structure or a potential for high permeability. In conclusion, the rock sample could be best described petrographically as a fine grained quartz sandstone (quartz arenite).

APPENDIX B

ROUGHNESS ANALYSIS PROGRAM , AND

SAMPLE OUTPUT FOR TEST #61

( Y. OHNISHI )

```

000002 PROGRAM MAIN (INPUT,OUTPUT)
000002 DETERMINATION OF MULTIPLE REGRESSIONS BY FITTING A LINEAR
C REGRESSION EQUATION
C DIMENSION X1(200),X2(200),B(3),A(3,4)
COMMON Y(61),YDIF(72),NX1,NX2,DX1
N IS NO. OF OBSERVATIONS
MP IS NO. OF COEFF. R(I)
DA1 IS A LENGTH OF INTERVAL
NA1 IS NO. OF INTERVALS IN THE DIR. OF X1
NA2 IS NO. OF INTERVALS IN THE DIR. OF X2
READ 101,N,MP
101 FORMAT(2I5)
READ 102,DX1
102 FORMAT(F10.5)
READ 104,NX1,NX2
104 FORMAT(2I5)
PRINT 100,N,MP
100 FORMAT(1H0,2X,*,NO. OF OBSERVATIONS = *,110,3X
1,*,NO. OF COEFF. B(I) = *,15,/)
PRINT 103,DX1
103 FORMAT(1H0,2A,*,LENGTH OF INTERVAL DX1 = *,F10.5,/)
PRINT 105, NX1,NX2
105 FORMAT(1H0,2A,*,NO. OF INTERVALS IN THE DIR. OF X1 = *,15,*,NO. 0
IF INTERVALS IN THE DIR. OF X2 = *,15,/)
PRINT 200
200 FORMAT(10X,4HY(I),10X,5HX1(I),10X,5HX2(I),5X,23HGRADIENT(SLOPE) OF
1 Y(I),/)
DO 10 I=1,N
READ 201,X1(I),Y(I),X2(I)
201 FORMAT(3F10.4)
10 CONTINUE
CALL SUBY
N2=0
N1=N-NX1+2
PRINT 202, Y(MM-1),X1(MM-1),X2(MM-1)
202 FORMAT(5X,F10.4,5X,F10.4,5X,F10.4)
DO 12 I=MM,MH1
PRINT 203,Y(I),X1(I),X2(I),YDIF(I-M-1)
203 FORMAT(5X,F10.4,5X,F10.4,5X,F10.4,5X,F10.4,10X,F10.4)
12 CONTINUE
N2=N2+1
IF(I.GE.N) GO TO 15
15 TX1=0.0
TX2=0.0
TSX1=0.0
TX12=0.0
TSX2=0.0
TY=0.0
TSY=0.0
TXY=0.0
TX2Y=0.0
INITIAL T MEANS TOTAL SUM OF VARIABLES
INITIAL TS MEANS TOTAL SUM OF SQUARES OF VARIABLES
DO 3J I=1,N
TAL=TAL+X1(I)
TAS=TAS+X2(I)

```

```

000164 TSX1=(SX1*X1(I)+X1(I))
000165 TX12=TX12+X1(I)*X2(I)
000167 TSX2=(SX2*X2(I)+X2(I))
000170 TY=TY+Y(I)
000172 TSY=(SY+Y(I))*Y(I)
000174 TXY=TX1Y+X1(I)*Y(I)
000175 TXY2=TX2Y+X2(I)*Y(I)
000177 30 CONTINUE
000204 A(1,1)=N
000205 A(2,1)=TX1
000206 A(3,1)=TX2
000210 A(2,2)=SX1
000211 A(3,2)=TX12
000213 A(3,3)=TSX2
000215 A(2,3)=A(3,2)
000216 A(1,3)=A(3,1)
000217 A(1,2)=A(2,1)
000220 L=NP+1
000222 A(1,L)=TY
000223 A(2,L)=TX1Y
000227 A(3,L)=TX2Y
000235 PRINT 249
000240 249 FORMAT(10X,'22HA MATRIX OF NORMAL EQ./././)
000240 PRINT 250,((A(I,J),J=1,L),I=1,NP)
000257 250 FORMAT(5X,'F15.5)
C
000257 DET=1.0
000260 M=NP+1
000262 I=1
000266 5 PIVOT=A(I,I)
000267 DET=DET*PIVOT
000271 A(I,1)=1.0
000272 J=1
000275 1 A(I,J)=A(I,J)/PIVOT
000301 J=J+1
000303 IF(J.LE.M) GO TO 1
000305 K=1
000306 4 IF(K.EQ.I) GO TO 2
000312 AMULT=A(K,I)
000312 A(K,1)=0.0
000313 J=1
000317 3 A(K,J)=A(K,J)-AMULT*A(I,J)
000326 J=J+1
000330 IF(J.LE.M) GO TO 3
000332 2 K=K+1
000334 4 IF(K.LE.NP) GO TO 4
000336 I=I+1
000337 IF(I.LE.NP) GO TO 5
C
000340 END OF INVERTING A MATRIX
000345 R(I)=0.0
000346 DO 35 I=1,3
000347 35 CONTINUE
000354 R(I)=A(1,L)
000357 40 CONTINUE
000360 SUMYR=0.0
000360 YRMAX=0.0
000361 YRMIN=0.0

```

```

000362      DO 41 I=1,N
000371      YRES=Y(I)-B(2)*X1(I)-B(3)*X2(I)
000376      SUMYRE=SUMYRE+YRES
000377      IF (YRES.GE.YRMAX) YRMAX=YRES
000402      IF (YRES.LE.YRMIN) YRMIN=YRES
000406      *1 CONTINUE
000407      YMAXDIF=YRMAX-YRMIN
000411      PRINT 270,YRMAX,YRMIN,YMAXDIF
000422      270 FORMAT(5X,'THE MAX. DIVIATION FROM THE MEAN PLANE*+ DIRECTION# * *
1,F10.5,X,'-DIRECTION# * *F10.5,*MAX.DIF. = *F10.5*/./)
000427      PRINT 271,SUMYRE
000430      271 FORMAT(5X,'THE SUM. OF RESIDUALS * *F15.7./)
000434      PRINT 299
000436      299 FORMAT(5X,'SDETERMINED REGRESSION PLANE OR LINE./)
000443      PRINT300,(B(I),I=1,NP)
000443      300 FORMAT(5X,'Y = *F15.5,* X1 *F15.5,* X2 *././)
C      ESQ IS THE SUM OF SQUARES OF RESIDUALS
000443      SSR=3(2)*(TX1-TX1*TY/N)+8(3)*(TX2-TX2*TY/N)
000443      ESQ=(TSY-TY*TY/N)-SSR
000443      SOS=ESQ/(N-3)
000443      STORES=SQRT(SOS)
000443      PRINT 500,ESQ,SOS
000443      500 FORMAT(5X,'THE SUM OF SQUARES OF RESIDUALS * *F15.5
1,* THE ESTIMATE OF SIGMA SQUARE * *F15.5./)
C      PRINT 501,STORES
000476      501 FORMAT(5X,'THE ESTIMATE OF STANDARD DIVIATION OF RESIDUALS * *
1,F15.7././)
C      *** CALCULATION OF DIF. Y(I) DISTRIBUTION ***
000504      YDIF=0.0
000505      TSYDIF=0.0
000506      SLOPOS=0.0
000506      SLONEG=0.0
000506      M1=0
000507      M2=0
000507      N1=N-NX2
000512      DO 50 I=1,N1
000514      TYDIF=TYDIF+YDIF(I)
000515      TSYDIF=TSYDIF+YDIF(I)
000517      IF (YDIF(I)) 53,52,51
000521      51 M1=M1+1
000523      SLOPOS=SLOPOS+YDIF(I)
000525      52 GO TO 50
000526      53 M2=M2+1
000530      SLONEG=SLONEG+YDIF(I)
000532      50 CONTINUE
000535      YDMEAN=TYDIF/(N1)
000536      STNDIV=SQRT(TSYDIF/(N1)-YDMEAN**2)
000544      SLP0AV=SLOPOS/M1
000546      SLNEAV=SLONEG/M2
000551      PRINT 550, SLP0AV
000556      550 FORMAT(5X,'THE AVERAGE OF SLOPE OF POSITIVE DIRECTION **F10.5./)
000556      PRINT 551, SLNEAV
000556      551 FORMAT(5X,'THE AVERAGE OF SLOPE OF NEGATIVE DIRECTION **F10.5./)
000564      PRINT 601,YDMEAN
000564      601 FORMAT(5X,'THE MEAN VALUE OF DISTRIBUTION OF SLOPE OR GRADIENT
1 = *F15.7./)
000572      PRINT 602, STNDIV
000572

```

000600 602 FOR-1A1(SX, \* THE STANDARD DIVIATION OF DISIRIBUTION OF SLOPE  
 000600 1 OH GRADIENT = \*.F15.7,/) STOP  
 000602 END

PROGRAM LENGTH INCLUDING I/O BUFFERS  
 006043

FUNCTION ASSIGNMENTS

STATEMENT ASSIGNMENTS	3	4	5	11	501
1 - 000274	3	4	5	11	501
15 - 000146	41	51	52	53	000103
100 - 000523	101	103	104	105	000527
200 - 000660	201	203	249	250	000644
270 - 000715	271	300	500	501	000711
550 - 001001	551	602	500	501	000770

BLOCK NAMES AND LENGTHS  
 = 000234

VARIABLE ASSIGNMENTS

VARIABLE	ASSIGNMENT	ASSIGNMENT	ASSIGNMENT	ASSIGNMENT	ASSIGNMENT
A	001712	AMULT	001752	R	001707
I	001730	J	00174	K	001751
MM1	001733	M1	00177J	L	001745
NX2	00232C01	N1	001772	N	001771
SLPOAV	001775	SOS	001762	SLNEAV	001750
TSX1	001736	TSX2	001740	STDRES	001760
TX2	001737	TX2	001735	TSYDIF	001742
X2	001377	Y	00000C01	TY	001744
YRMAX	001754	YRMIN	001755	TYDIF	001741
				YDIF	001773
				YDMEAN	00121C01
				DET	001707
				L	001751
				N	001771
				PIVOT	001750
				SSR	001760
				TSY	001742
				TX2Y	001744
				YDIF	00000C01
				YRMIN	001755
				DX1	00233C01
				M	001731
				NP	001727
				SLOMEG	001767
				STNDIV	001774
				TX1	001734
				TYDIF	001764
				YMAXDIF	001757
				ES0	001761
				M4	001732
				NX1	000231C01
				SLOPOS	001766
				SUMYRE	001753
				TX1Y	001743
				X1	001067
				YRES	001756

START OF COVSTANTS--000605 TEMPS--001045 INDIRECTS--001061

ROUTINE COMPILES IN 043500

TEST # 61 - GRANITE FILLED, ROUGHNESS 4

NO. OF OBSERVATIONS = 81 NO. OF COEFF. B(I) = 3

LENGTH OF INTERVAL  $\Delta X_1 = .50000$

NO. OF INTERVALS IN THE DIP. OF X1 = 9 NO. OF INTERVALS IN THE DIP. OF X2 = 9

Y(I) X1(I) X2(I) GRADIENT(SLOPE) OF Y(I)

.0701	0.	0.	
.0555	.0500	0.	.0728
.0550	.1000	0.	-.0012
.2773	.1500	0.	-.0552
.2114	.2000	0.	-.0378
.2039	.2500	0.	.1050
.2337	.3000	0.	-.0264
.2304	.3500	0.	.0594
.2223	.4000	0.	.0918
.3595	0.	.0500	
.2929	.0500	.0500	-.0132
.3153	.1000	.0500	.1278
.2035	.1500	.0500	-.2246
.2627	.2000	.0500	.1168
.2073	.2500	.0500	.0878
.1359	.3000	.0500	-.0088
.2757	.3500	.0500	-.0352
.3033	.4000	.0500	.0360
.3331	0.	.1000	
.3133	.0500	.1000	.1544
.2775	.1000	.1000	.1692
.2923	.1500	.1000	-.2344
.2077	.2000	.1000	.0634
.2737	.2500	.1000	-.0276
.2741	.3000	.1000	-.0112
.2032	.3500	.1000	-.0173
.3115	.4000	.1000	.0226
.3033	0.	.1500	
.2250	.0500	.1500	.0903
.3775	.1000	.1500	.3978
.2117	.1500	.1500	-.3312
.2023	.2000	.1500	.1470
.2073	.2500	.1500	.0240
.2732	.3000	.1500	-.0360
.2717	.3500	.1500	.0412
.2725	.4000	.1500	-.0578
.2761	0.	.2000	
.2015	.0500	.2000	.0908
.2073	.1000	.2000	.2510
.3747	.1500	.2000	-.1646

Reproduced from  
best available copy.

Reproduced from  
 Best available copy.

.1672	.2000	.2000	-.3150
.3122	.2500	.2500	.2700
.2927	.3000	.2000	-.1190
.2106	.3500	.2000	-.0638
.2762	.4000	.2000	.1270
.2677	0.	.2500	.2250
.3192	.1500	.2500	-.1416
.3094	.1000	.2500	.0760
.3676	.1500	.2500	-.2130
.2609	.2000	.2500	.1176
.2317	.2500	.2500	-.1776
.2104	.3000	.2500	.0793
.2733	.3500	.2500	.0916
.2163	.4000	.2500	.1402
.2714	0.	.3000	-.0560
.3582	.0500	.3000	-.0072
.3175	.1000	.3000	-.2802
.3173	.1500	.3000	.1314
.2633	.2000	.3000	-.3560
.2100	.2500	.3000	.2474
.2100	.3000	.3000	.0134
.1335	.3500	.3500	-.0152
.1335	.4000	.3500	.1310
.2624	.4500	.3500	.0656
.2021	.5000	.3500	-.2810
.3393	0.	.3500	-.0248
.2014	.0500	.3500	-.0132
.2014	.1000	.3500	.0576
.2014	.1500	.3500	.0378
.2014	.2000	.4000	.0180
.2014	.2500	.4000	.0524
.2014	.3000	.4000	.0196
.2014	.3500	.4000	-.2630
.2014	0.	.4000	-.1756
.2014	.0500	.4000	.1950
.2014	.1000	.4000	.0814
.2014	.1500	.4000	.0316

THE MAX. DEVIATION FROM THE MEAN PLANE\*+ DIRECTION# = .12023    \*-DIRECTION# = -.16395\*MAX.DIF. = .26408

THE SUM OF RESIDUALS = .0000000  
 OFF CENTERED REGRESSION PLANE OR LINE  
 Y = .2118    -.04709 X1    .04993 X2

THE SUM OF SQUARES OF RESIDUALS = .29760 THE ESTIMATE OF SIGMA SQUARE = .00266

THE ESTIMATE OF STANDARD DEVIATION OF RESIDUALS = .0515903 THIS IS THE ROUGHNESS

THE AVERAGE OF SLOPE OF POSITIVE DEFLECTION = .10595

THE AVERAGE OF SLOPE OF NEGATIVE DIRECTION = -.11743

THE MEAN VALUE OF DISTRIBUTION OF SLOPE OR GRADIENT = .0697722

THE STANDARD DEVIATION OF DISTRIBUTION OF SLOPE OR GRADIENT = .1413418

Reproduced from  
best available copy.

## APPENDIX C

WAVINESS ANALYSIS PROGRAM , AND

SAMPLE OUTPUT FOR TEST #61

( Y. OHNISHI )

```

000073 PROGRAM MAIN (INPUT,OUTPUT)
000074 DIMENSION X(1200),X2(200), DX(8),MED(8),Y(172)
000075 INTEGER M(82),M(80)
000076 DATA W(80) /M(82),M(80) /
000077 COMMON V(81),Y(172),X(1),X2(1),DX(1)
000078 M IS NO. OF OBSERVATIONS
000079 N IS NO. OF COEFF. IN I
000080 DX(1) IS A LENGTH OF INTERVAL HAD AFTER READ
000081 X(1) IS NO. OF INTERVALS IN THE DIR. OF X1
000082 X2(1) IS NO. OF INTERVALS IN THE DIR. OF X2
000083 READ 101,N,M
000084 IF (M(81)-EQ-M(80)) GO TO 7
000085 IF (M(81)-EQ-M(80)) STOP
000086 GO TO 6
000087 READ 107,MED
000088 PRINT 109
000089 PRINT 106,MED
000090 PRINT 100,N,DX(1)
000091 READ 301,(Y(I),I=1,N)
000092 CALL SUBV
000093 DO 11 K=1,8
000094 PRINT 400, DX(K)
000095 J=1
000096 M=1
000097 DO 12 M=(M-1)+8+1
000098 M1=8*M
000099 Y(1)=0.2
000100 M1=M1-1
000101 DO 13 I=M1,M1+M
000102 Y(I)=Y(I)+Y(I)
000103 PRINT 110
000104 Y(172)=Y(1)+Y(1)
000105 Y(171)=Y(1)+Y(1)
000106 J=J+1
000107 M=M+1
000108 IF (M(81)-LT-M(80)) GO TO 13
000109 IF (M(81)-EQ-M(80)) GO TO 15
000110 M=1
000111 GO TO 12
000112 DO 15 L=(L+1)+DX(1)-K
000113 PRINT 1000 ,(Y(172),I=1,L)
000114 Y(1)=0
000115 Y(172)=0
000116 Y(171)=0
000117 Y(170)=0
000118 M1=0
000119 M2=0
000120 DO 16 I=1,L

```

Reproduced from  
best available copy.

```

000332 IF(YD1(I)) 53,52,51
000334 51 M1=M1+1
000336 SLOPOS=SLOPOS+YD1(I)
000340 92 GO TO 50
000341 53 M2=M2+1
000343 SLONEG=SLONEG+YD1(I)
000345 IF(YD1(I).GE.YDMAX) YDMAX=YD1(I)
000347 IF(YD1(I).LE.YDMIN) YDMIN=YD1(I)
000357 16 CONTINUE
000362 IF(M1.EQ.0) M1=123
000364 IF(M2.EQ.0) M2=456
000366 SLOPAV=SLOPOS/M1
000368 SLINEAV=SLONEG/M2
000370 SPD=180.0*ATAN(SLOPAV)/3.14
000372 SND=180.0*ATAN(SLINEAV)/3.14
000374 YDMDG=180.0*ATAN(YDMAX)/3.14
000376 YDMIDG=180.0*ATAN(YDMIN)/3.14
000378 PPINT 550,SLOPAV,SPD
000380 PRINT 2000,YDMAX,YDMDG,YDMIN,YDMIDG
000382 11 CONTINUE
000384 GO TO 6
000386 100 FORMAT(IHO,2X,* NO. OF OBSERVATIONS = *,I10,2X
000388 1,* LENGTH OF INTERVAL HAD BEEN READ,DX1 = *,F10.5,////)
000390 101 FORMAT(2I5)
000392 102 FORMAT(F10.5)
000394 104 FORMAT(2I5)
000396 106 FORMAT(A6)
000398 107 FORMAT (8I9)
000400 108 FORMAT (8A9)
000402 109 FORMAT (1H1)
000404 110 FORMAT (8F5.0)
000406 201 FORMAT (14F5.2)
000408 101 FORMAT (7F10.5)
000410 400 FORMAT (15X,* WAIVNESS ON SCALE OF *,F5.2,* INCH *)
000351 551 FORMAT(5X,* THE AVERAGE OF SLOPE OF POSITIVE DIRECTION =*,F10.5,2X
1,* THE AVE. POS. SLOPE ANGLE=*,F6.1,* DEGREES*)
000351 551 FORMAT(5X,* THE AVERAGE OF SLOPE OF NEGATIVE DIRECTION =*,F10.5,2X
1,* THE AVE. NEG. SLOPE ANGLE=*,F6.1,* DEGREES*)
000351 1000 FORMAT(12F10.5)
000351 2000 FORMAT(
1,*MIN,NEG.SLOPE=*,F8.5,2X,*MAX,POS.ANGLE=*,F6.1,2X
1,*MIN,NEG.SLOPE=*,F8.5,2X,*MIN,NEG.ANGLE=*,F6.1,/)
000351 FND

```



FORTRAN COMPILER VERSION 2.3 B.2

```
000002 SUBROUTINE SUBY  
000003 COMMON YY(9,9),YD(8,9),NX1,NX2,DX1  
000004 NN1=NX1-1  
000005 DO 111 J=1,NX2  
000006 DO 111 I=1,NN1  
000007 YD(I,J)=(YV(I+1,J)-YV(I,J))/DX1  
000008 111 CONTINUE  
000009 RETURN  
000010 END
```

NO. OF OBSERVATIONS = 81 LENGTH OF INTERVAL HAD BEEN READ, DX1 = .50000

RAVINESS ON SCALE OF .50 INCH  
 .07283 -.00120 -.05620 -.03280 .10900  
 .08490 -.00850 -.03520 .03680 .16440  
 .09083 .04780 .03170 .14780 .02400  
 .27033 .11900 .06380 .12700 .22500  
 .14823 .06700 .00720 .26020 .13360  
 .32483 .01320 .05760 .08780 .01800  
 THE AVERAGE OF SLOPE OF POSITIVE DIRECTION =  
 THE AVERAGE OF SLOPE OF NEGATIVE DIRECTION =  
 MAX.POS.SLOPE= .27000 MAX.POS.ANGLE= 15.1 MIN.NEG.SLOPE= -.34400 MIN.NEG.ANGLE= -19.0  
 THE AVE. POS. SLOPE ANGLE= 6.1 DEGREES  
 THE AVE. NEG. SLOPE ANGLE= -6.7 DEGREES

RAVINESS ON SCALE OF 1.00 INCH  
 .03590 -.02870 .04450 .03910 .03930  
 .02200 .00040 .16670 .06370 .10400  
 .08590 .00500 .00360 .03830 .17090  
 .03280 .06850 .04770 .03000 .04890  
 .13060 .04340 .12380 .11070 .13880  
 .00920 .13820 .05650  
 THE AVERAGE OF SLOPE OF POSITIVE DIRECTION =  
 THE AVERAGE OF SLOPE OF NEGATIVE DIRECTION =  
 MAX.POS.SLOPE= .17000 MAX.POS.ANGLE= 9.7 MIN.NEG.SLOPE= -.23980 MIN.NEG.ANGLE= -13.5  
 THE AVE. POS. SLOPE ANGLE= 3.6 DEGREES  
 THE AVE. NEG. SLOPE ANGLE= -3.8 DEGREES

RAVINESS ON SCALE OF 1.50 INCH  
 .00513 -.00307 .00533 .01527 .04600  
 .01233 -.01300 .01653 .01653 .01887  
 .05907 .07620 .06987 .05467 .02907  
 .05900 .06713 .04467 .15693 .01240  
 .03000 .00300 .07333 .01487 .03327  
 THE AVERAGE OF SLOPE OF POSITIVE DIRECTION =  
 THE AVERAGE OF SLOPE OF NEGATIVE DIRECTION =  
 MAX.POS.SLOPE= .10267 MAX.POS.ANGLE= 5.9 MIN.NEG.SLOPE= -.15693 MIN.NEG.ANGLE= -8.9  
 THE AVE. POS. SLOPE ANGLE= 1.8 DEGREES  
 THE AVE. NEG. SLOPE ANGLE= -2.7 DEGREES

RAVINESS ON SCALE OF 2.00 INCH  
 .00435 .00370 .00260 .02630 .05745  
 .06170 .00795 .00900 .00130 .01540  
 .05355 .01340 .04025 .04925 .04830  
 .01630 .06485 .06710 .02685 .00675  
 THE AVERAGE OF SLOPE OF POSITIVE DIRECTION =  
 THE AVERAGE OF SLOPE OF NEGATIVE DIRECTION =  
 MAX.POS.SLOPE= .03745 MAX.POS.ANGLE= 3.3 MIN.NEG.SLOPE= -.11950 MIN.NEG.ANGLE= -6.8  
 THE AVE. POS. SLOPE ANGLE= 1.3 DEGREES  
 THE AVE. NEG. SLOPE ANGLE= -2.1 DEGREES

RAVINESS ON SCALE OF 2.50 INCH  
 .01752 .00232 .00980 .03940 .01932  
 .00988 .01912 .03064 .02424 .02844  
 .02020 .00152 .01240 .03972 .01956  
 .00152 .00152 .00152 .00152 .00152  
 .02016 .01280 .01556 .06772 .05292  
 .02036 .02036 .02036 .02036 .02036

.01604 --.08240 --.04604 --.04192 --.03188 --.01568 --.04036 --.03612 --.02992 .00548 .01128 .01368  
 THE AVERAGE OF SLOPE OF POSITIVE DIRECTION = .01914 THE AVE. POS. SLOPE ANGLE = 1.1 DEGREES  
 THE AVERAGE OF SLOPE OF NEGATIVE DIRECTION = -.03414 THE AVE. NEG. SLOPE ANGLE = -2.0 DEGREES  
 MAX.POS.SLOPE = .03972 MAX.POS.ANGLE = 2.3 MIN.NEG.SLOPE = -.08240 MIN.NEG.ANGLE = -4.7

WAVINESS ON SCALE OF 3.00 INCH

.01020 .00787 .02347 .01463 .01097 --.00433 .01443 --.01593 --.02867 --.00080 --.00907 --.00347 --.03500  
 .07220 --.02357 --.04423 --.01893 --.04313 --.00430 --.04397 --.02737 --.03613 --.02877 --.00347 --.00347 --.01900  
 .00757 .01813 .01457  
 THE AVERAGE OF SLOPE OF POSITIVE DIRECTION = .01242 THE AVE. POS. SLOPE ANGLE = .7 DEGREES  
 THE AVERAGE OF SLOPE OF NEGATIVE DIRECTION = -.02275 THE AVE. NEG. SLOPE ANGLE = -1.3 DEGREES  
 MAX.POS.SLOPE = .02347 MAX.POS.ANGLE = 1.3 MIN.NEG.SLOPE = -.04423 MIN.NEG.ANGLE = -2.5

WAVINESS ON SCALE OF 3.50 INCH

.01723 .01794 .00751 .01454 .00583 --.00043 .00520 --.01603 --.00723 --.00206 --.00483 --.02391  
 --.00229 --.02154 --.01643 .00957 .01811 .02006  
 THE AVERAGE OF SLOPE OF POSITIVE DIRECTION = .01356 THE AVE. POS. SLOPE ANGLE = .8 DEGREES  
 THE AVERAGE OF SLOPE OF NEGATIVE DIRECTION = -.01053 THE AVE. NEG. SLOPE ANGLE = -.6 DEGREES  
 MAX.POS.SLOPE = .02006 MAX.POS.ANGLE = 1.1 MIN.NEG.SLOPE = -.02391 MIN.NEG.ANGLE = -1.4

WAVINESS ON SCALE OF 4.00 INCH

.02655 .01108 .02018 --.03267 .00955 .00720 --.00033 --.00340 .01980  
 THE AVERAGE OF SLOPE OF POSITIVE DIRECTION = .01572 THE AVE. POS. SLOPE ANGLE = .9 DEGREES  
 THE AVERAGE OF SLOPE OF NEGATIVE DIRECTION = -.00213 THE AVE. NEG. SLOPE ANGLE = -.1 DEGREES  
 MAX.POS.SLOPE = .02655 MAX.POS.ANGLE = 1.5 MIN.NEG.SLOPE = -.00340 MIN.NEG.ANGLE = -.2

APPENDIX D

TYPICAL TEST RECORD ( TEST # 61 )

UNIVERSITY OF CALIFORNIA  
ROCK MECHANICS LABORATORY

Direct Shear Test

Date: \_\_\_\_\_ Accession Number: \_\_\_\_\_  
 Operator: Heuzé / Ohnishi Test Series or Sponsor: ARPA 1971-1972  
 Series Number: # 61

Sample Description

Rock Type      GRANITE  
 Size            4.75 \* 4.75 in.

Discontinuity Description

Type of Joint    Filled  
 Comment        Roughness 4 (Split)

Filling Material    Kaolinite                      (mm)                      (in)  
 Thickness        7.2 \* 10<sup>-2</sup> in.  
 Preconsolidation pressure    100 psi

Shear Rate        #1 (L 50)                      in/min :0.1

Back Pressure P<sub>b</sub>    200 psi

Normal Pressure at Start of Virgin Shear Test

Accumulator pressure (psi)  
 Normal force (lbs)  
 Normal stress (psi)    500 psi

ROUGHNESS MEASUREMENTS

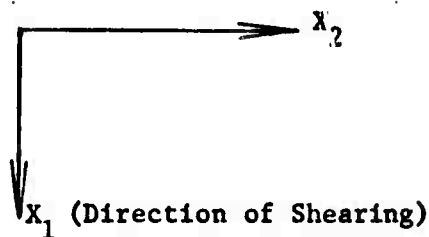
Shear Test Number

Test Series

Number in Series

ARPA 1971-1972

# 61



Date

Operator

Grid Size

Heuzé

0.5 in.

.2201	.2595	.2308	.2832	.2361	.2677	.2704	.3055	.2720
.2565	.2529	.3130	.3286	.2815	.3802	.3445	.2584	.2810
.2559	.3168	.3975	.3775	.4070	.3094	.3775	.3489	.3072
.2278	.2045	.2493	.2119	.3247	.3474	.3739	.3822	.3170
.2114	.2629	.2935	.2858	.1672	.2409	.2438	.2382	.2855
.2639	.3078	.2797	.2978	.3022	.2997	.3105	.2258	.1972
.2507	.3034	.2741	.2808	.2427	.2109	.1385	.2192	.2947
.2804	.2858	.2652	.3014	.2108	.2508	.2624	.2480	.3354

.3263    .3038    .3115    .2725    .2743    .2965    .2691    .2919    .3512

Log of Direct Shear Test XYY' Record

Test Accession No.

ARPA 1971-1972 # 61

<u>Subtest 1 (Reading numbers: )</u>				
	Channel	Name of Variable	Volts/inch	1 inch =:
X	1	$\sigma_n$	0.10	2,060 lbs
Y <sub>1</sub>	6	v	0.05	$5.63 \times 10^{-3}$ in.
Y <sub>2</sub>	7	u	0.01	$4.0 \times 10^{-3}$ in.
<u>Subtest 2 (Reading numbers: )</u>				
			<u>X-Y-Y' #1</u>	<u>X-Y-Y' #2</u>
X	5	P	0.10	P Scale 2
Y <sub>1</sub>	6	v	0.05	p <sub>1</sub> Scale 2
Y <sub>2</sub>	7	u	0.01	p <sub>2</sub> Scale 2
<u>Subtest 3 (Reading numbers: )</u>				
				<u>X-Y-Y' #1</u>
X	2	$\tau$	0.10	2,060 lbs
Y <sub>1</sub>	6	v	0.05	$5.63 \times 10^{-3}$ in.
Y <sub>2</sub>	7	u	0.05	$2.0 \times 10^{-2}$ in.
<u>Subtest 3 (Reading numbers: )</u>				
				<u>X-Y-Y' #2</u>
X	2	$\tau$	Scale 1	
Y <sub>1</sub>	3	P <sub>1</sub>	Scale 5	
Y <sub>2</sub>	4	P <sub>2</sub>	Scale 5	

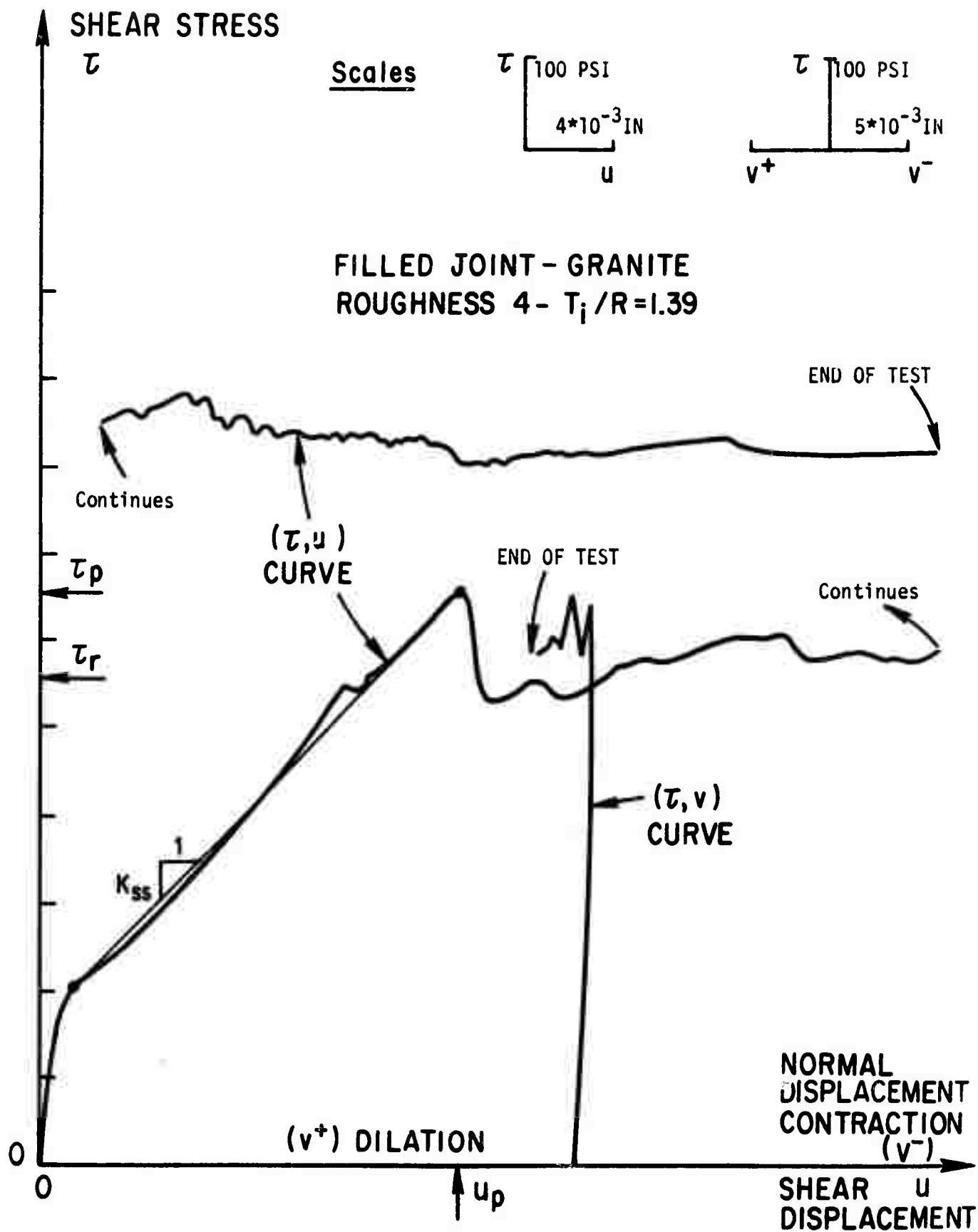


FIGURE 25 : RECORD OF TEST # 61